A CFD – FEA CO-SIMULATION TO INVESTIGATE THE EFFECTS OF THERMAL BARRIER COATINGS ON GASOLINE COMPRESSION IGNITION COMBUSTION

A Thesis
Presented to the
Graduate School of
Clemson University

In Partial Fulfillment of the
Requirements for the Degree
Master of Science
Automotive Engineering

---

by
Prakash Koirala
April 2024

Committee:
Dr. Benjamin Lawler, Committee Chair
Dr. Zoran Filipi
Dr. Brian Gainey

ABSTRACT

Thermal barrier coatings (TBCs) have the potential to reduce heat transfer losses from engines and thereby improve engine efficiency. TBCs might also help address issues related to advanced combustion strategies including low-temperature combustion (LTC). Therefore, this thesis investigates how TBCs affect gasoline compression ignition (GCI), an advanced combustion strategy, using state-of-the-art modeling techniques. TBCs are used in gas turbine engines to block heat transfer to the turbine blades to improve their efficiency and mechanical reliability. As a result, there have been numerous research studies into the use of TBCs in internal combustion engines, which is still an active area of research. GCI combustion is a new, advanced combustion strategy that is both efficient and produces low emissions. In this study, we used a coating material called Gadolinium Zirconate (Gd-Zr) TBC on the piston of a GCI engine running at 1500rpm and at three different operating conditions of 6-bar, 10-bar, and 15-bar. The goal was to use modeling to determine how this coating affects the engine's performance. We found that the TBC made the engine's surface temperature swing more than 100K, and this helped reduce heat loss from the gas to the walls, making the engine more efficient. A coupled modeling of CFD and FEA to simultaneously analyze fluid flow and structural behaviors under various conditions was used until a quasi-steady state was achieved. This integrated approach allows for a comprehensive evaluation of both the thermal and mechanical performance of materials and components in a simulated environment, such as assessing the heat distribution within an engine coated with TBCs.

This thesis studies the thermal performance of the TBCs, but these modeling techniques could be used to study the mechanical performance of the TBCs in the future if desired. The computer simulations using CFD and FEA predicted that the TBC coating could improve efficiency by about 0.5 percentage points compared to an uncoated metal engine for all three

operating conditions. However, when these TBCs were tested experimentally in real engines, a different trend emerged wherein there was an slight efficiency improvement at the low loads that matched the CFD-FEA results, but there was a slight efficiency penalty at the highest load, which did not agree with the CFD-FEA results. A possible reason for this difference is the theory of "convection vive", which is a phenomenon where combustion occurring in the near-wall thermal boundary layer causes the convective heat transfer coefficient to increase. Convection vive is not currently captured by CFD submodels, which might explain the discrepancy between the modeling results and the experiments. Future work could determine how convection vive, or any other uncaptured physical phenomena, could be included in the computer predictions to improve their accuracy. A more advanced direct numerical simulation (DNS) study could help by effectively capturing the near-wall thermal conditions and combustion reactions.

ACKNOWLEDGEMENTS

I want to thank Dr. Benjamin Lawler for being not just a mentor in my studies, but also a friend who supported me through these two years of learning and growth. Even though I'm far from home, Dr. Lawler has been there to encourage me and make me feel welcome. His kindness and passion have helped me gain confidence and enjoy my time here.

I also want to thank Dr. Zoran Filipi for keeping me focused and motivated. I'm grateful for the guidance and support from Dr. Brian Gainey for his help with the thermal barrier coating experiments. I'm thankful to my colleagues Rahul Motwani, Avinash Ravikumar, Kunal Vedpathak, and Mohit Kumar for their teamwork and friendship. I owe a lot to my parents for their love and support, and for always being there for me.

I would gratefully like to acknowledge Clemson University's Cyberinfrastructure Technology Integration (CITI) group for providing computational resources through the Palmetto supercomputing cluster, as well as CONVERGE for providing their CFD software. The authors would also like to thank Aramco Services Company (ASC) and Solution Spray Technologies (SST) for providing the piston and necessary coatings to the experiment.

TABLE OF CONTENTS

LIST OF TABLES

LIST OF FIGURES

LIST OF ABBREVIATIONS

AMR	Adaptive Mesh Refinement
aTDC	After Top Dead Center
BCs	Boundary Conditions
CAD	Computer Aided Design
CFD	Computational Fluid Dynamics
CHT	Conjugate Heat Transfer
DNS	Direct Numerical Simulation
EVC	Exhaust Valve Closing
EVO	Exhaust Valve Opening
GCI	Gasoline Compression Ignition
GdZr	Gadolinium Zirconate
GDI	Gasoline Direct Injection
HTC	Heat Transfer Coefficient
HRR	Heat Release Rate
IC	Internal Combustion
IMEP	Indicated Mean Effective Pressure
ISFC	Indicated Specific Fuel Consumption
IVC	Intake Valve Closing
IVO	Intake Valve Opening
LES	Large Eddy Simulation
RNG	Renormalization Group

RANS	Reynold's Averaged Navier Stoke
RPM	Revolution per Minute
SI	Spark Ignition
SOI	Start of Injection
TBC	Thermal Barrier Coating
TWT	Transient Wall Temperature
YSZ	Yttria Stabilized Zirconia

CHAPTER ONE

INTRODUCTION

1.1.Thermal Barrier Coatings

Thermal barrier coatings (TBCs) are advanced materials applied to internal combustion engine components to reduce heat transfer, enhancing performance, efficiency, and durability. By insulating critical areas like combustion chambers and exhaust systems, TBCs minimize heat transfer, maintaining lower temperatures and improving combustion efficiency while reducing thermal stress. This increases fuel economy, reduced emissions, and longer component life [1]. Thermal barrier coatings have emerged as a pivotal technology in enhancing the efficiency and performance of internal combustion (IC) engines, particularly in the realm of gasoline compression ignition (GCI) engines. These coatings applied to engine components such as pistons and combustion chambers, play a critical role in managing the engine's thermal environment. By reducing thermal conductivity, TBCs elevate in-cylinder temperatures, which in turn minimizes heat loss during the combustion process [2]. This thermal management strategy not only improves combustion stability, especially at low loads, but also significantly boosts the engine's indicated thermal efficiency.

In the context of GCI engines, which are known for their potential in achieving high thermal efficiency alongside low emissions, addressing the challenge of stable compression combustion at low loads is of greatest importance. TBCs address this by insulating the engine's critical components, thus maintaining higher operational temperatures. Experimental studies have shown that employing TBCs, particularly on the piston top surface and within the combustion chamber, can lead to a notable improvement in combustion efficiency and emissions reduction.

Specifically, at low load conditions, the application of TBCs has been demonstrated to increase indicated thermal efficiency by approximately 6.4% while concurrently reducing emissions of total hydrocarbons (THC) and carbon monoxide (CO) [1-3].

Thermal barrier coatings (TBCs), specifically yttria-stabilized zirconia (YSZ), have revolutionized the performance, efficiency, and emissions profile of Homogeneous Charge Compression Ignition (HCCI) engines [4]. HCCI engines, known for their ability to combine high efficiency with low emissions, rely heavily on the precise control of in-cylinder temperatures to initiate combustion at just the right moment. The introduction of TBCs offers a transformative approach to managing these critical temperatures, significantly influencing the combustion process. YSZ coatings, applied to engine components such as pistons, serve as thermal insulators, reducing heat loss during the combustion phase. This characteristic of TBCs is pivotal, as it allows for a more controlled and efficient burn, reducing unburnt hydrocarbons and carbon monoxide emissions while simultaneously improving thermal efficiency. Essentially, these coatings create a dynamic environment within the combustion chamber that adapts throughout the engine cycle. During intake, the coating prevents excessive heat absorption by the incoming charge, maintaining optimal charge density and volumetric efficiency. Figure 1 shows the surface temperature profiles for uncoated and coated pistons. During combustion, it minimizes heat transfer to the engine walls, ensuring that more energy is converted into useful work [4, 5].

The application process of these coatings, such as air plasma spray for YSZ, results in a thin yet effective insulating layer on the piston tops. This modification has been shown to advance autoignition, reduce combustion duration, and enhance overall engine performance. For instance, experiments with YSZ-coated pistons in single-cylinder HCCI engines have demonstrated tangible benefits, including the advancement of the autoignition point and reduced combustion durations.

These improvements lead to a decrease in hydrocarbon and carbon monoxide emissions, marking a significant step forward in the quest for cleaner and more efficient internal combustion engines [4, 6].

Moreover, the strategic application of TBCs opens new path for engineering combustion processes that are more resilient to variations in operational conditions. By fostering a more complete combustion and reducing emissions, TBCs align with the broader objectives of enhancing engine efficiency and reducing environmental impact. This innovative use of TBCs in HCCI engines represents not just a technical advancement, but a leap towards realizing engines that can meet the stringent demands of modern transportation – engines that are both highly efficient and environmentally friendly [7, 8].

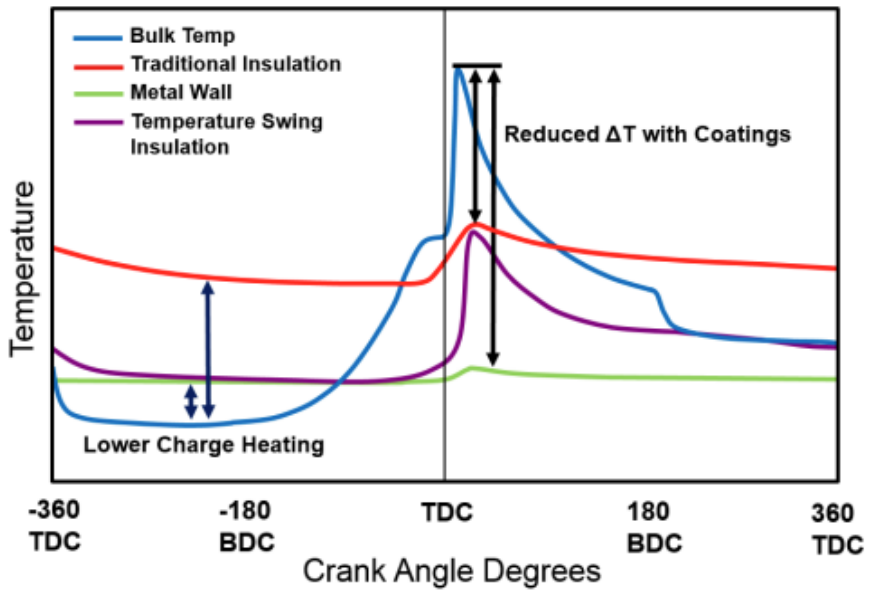

Figure 1: Surface temperature profiles for uncoated and coated pistons [9]

The exploration of TBCs in GCI is not just about emissions reduction; it's also about enhancing engine efficiency. TBCs, through their insulating properties, help to maintain higher temperatures within the combustion chamber. This, in turn, leads to more complete fuel

combustion, thereby reducing unburned hydrocarbons and carbon monoxide emissions. One notable aspect of TBCs is their ability to adapt to the dynamic thermal conditions of GCI engines. They minimize heat loss during the combustion process, which is crucial for maintaining the thermal efficiency of the engine. This thermal management is particularly beneficial at low and medium loads, where the potential for efficiency gains is significant [10].

Recent studies have presented the performance of TBCs under various GCI combustion conditions, focusing on how these coatings influence combustion efficiency and emissions across a range of operating loads. At lower loads, TBC-coated pistons have shown promising results in enhancing net fuel conversion efficiency and thermal efficiency, indicative of their potential to optimize engine performance. However, the benefits tend to diminish as the engine load increases, highlighting the complexity of thermal management [6].

The distinct behavior of TBCs in GCI also extends to their impact on emissions. While TBCs contribute to lower NOx and particulate matter emissions due to improved combustion efficiency, the interplay between coating characteristics (such as porosity and thermal inertia) and combustion dynamics can lead to variations in unburned hydrocarbons and CO emissions. This underscores the importance of tailoring TBC properties to the specific requirements of GCI combustion, aiming for a balance between thermal insulation and combustion efficiency [6, 10].

1.2. Gasoline Compression Ignition (GCI) Combustion

Gasoline compression ignition combustion mode is an advanced engine combustion strategy that combines the principles of both conventional spark ignition (SI) and diesel compression ignition (CI) combustion modes. It represents a transformative approach in the development of internal combustion engines, particularly for achieving high efficiency and reduced emissions in heavy-duty diesel engines. By utilizing the characteristics of gasoline - notably its lower reactivity

compared to diesel - GCI technology facilitates a combustion process that combines the high efficiency of diesel engines with significantly reduced emissions. GCI operates by compressing air within the cylinder to high temperatures, then injecting gasoline which auto-ignites due to the high air temperature [11]. This process benefits from gasoline's properties to achieve a more homogeneous air-fuel mixture before ignition, leading to a cleaner combustion process. The lower reactivity of gasoline, compared to diesel, allows for more controlled and gradual combustion, reducing the formation of soot and nitrogen oxides (NOx), which are common pollutants associated with diesel engines [11, 12, 13].

Experimental studies on GCI have focused on optimizing the combustion process to maximize efficiency while minimizing emissions. This involves intricate adjustments to the engine's compression ratio, the design of the piston bowls, and the timing and strategy of fuel injection. For instance, engines designed for GCI combustion have experimented with different piston designs such as wave and stepped-lip pistons to enhance mixing and combustion efficiency. These designs aim to manipulate the in-cylinder flow and the interaction between the injected fuel and the air, promoting better oxidation of soot particles and reducing heat losses [14, 15, 16].

Unlike conventional diesel engines, where combustion primarily depends on fuel-air mixing controlled by injection timing, GCI engines introduce a mix of kinetically controlled (premixed) and mixing-controlled combustion phases. This hybrid strategy harnesses gasoline's volatility and lower soot-forming potential to achieve cleaner combustion, while simultaneously exploring kinetically controlled combustion to limit NOx formation. Figure 2 shows the temperature and equivalence ratio map for soot and NOx formation. One of the key challenges in GCI technology is managing the low reactivity of gasoline [15, 16]. This challenge is met by creating conditions within the engine cylinder that promote efficient combustion despite gasoline's reluctance to ignite

under compression. Techniques such as advanced injection strategies, intake temperature management, and the incorporation of exhaust gas recirculation (EGR) are employed to control the combustion process [16]. These strategies not only ensure robust ignition but also allow for a wider operating range compared to traditional Homogeneous Charge Compression Ignition (HCCI) modes, which are constrained by the difficulties in managing ignition timing and combustion stability across different load and speed conditions [15, 16].

Moreover, the integration of TBCs with GCI engines has been identified as a promising avenue for further enhancing combustion efficiency. TBCs are engineered materials applied to combustion chamber surfaces, including pistons and cylinder heads, to reduce heat transfer losses [17]. By maintaining higher temperatures within the combustion chamber, TBCs contribute to a more complete fuel burn, thus improving thermal efficiency and reducing emissions. Research has shown that the application of TBCs, specifically those with low thermal inertia, can significantly influence GCI combustion outcomes. These coatings not only mitigate heat loss during the expansion stroke but also help manage charge heating, making them an integral component in the pursuit of optimizing GCI engine performance [16, 17, 18].

Experimentation and research into GCI have shown that these engines can achieve combustion efficiencies comparable to or even exceeding those of traditional diesel engines across various loads, without the need for high injection pressures or complex after-treatment systems for emissions control [18, 19, 21]. The ignition delay, critical in GCI combustion, has been linked closely with the fuel's Research Octane Number (RON), highlighting the importance of fuel autoignition properties in achieving the desired combustion characteristics. Studies have demonstrated that fuels with similar Octane Indices (OIs), regardless of their RON or Motor

Octane Number (MON), exhibit comparable ignition delays and therefore similar combustion and emissions behavior in GCI engines [18, 19, 20].

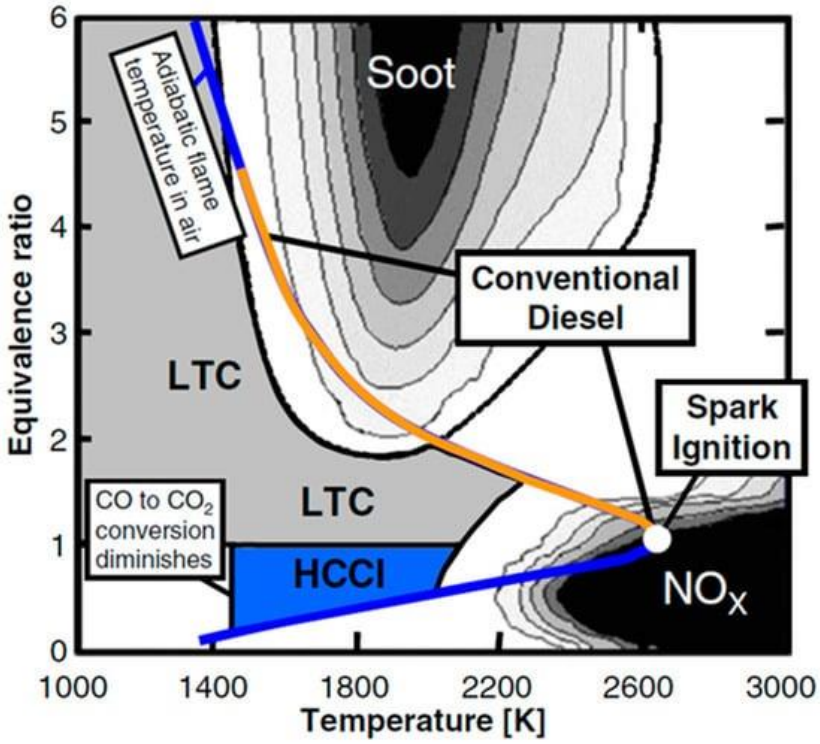

Figure 2: Temperature and equivalence ratio map for soot and NOx formation [22]

The "optimum" GCI fuel is thus one that requires less refining, is more readily available, and has a lower environmental impact than conventional gasoline or diesel. GCI engines can operate efficiently on these fuels over a broad range of conditions by adjusting engine parameters such as compression ratio, intake temperature, and exhaust gas recirculation (EGR) rates to manage the ignition delay and ensure optimal combustion [21, 23, 24].

The challenges of GCI combustion primarily revolve around managing the lower reactivity of gasoline, necessitating higher compression ratios or the use of additives to ensure reliable ignition and efficient combustion across various engine loads and speeds. Moreover, the variation

in gasoline composition can affect its reactivity, posing additional challenges for consistent engine performance [14, 16].

Despite these challenges, GCI technology presents a promising pathway toward cleaner and more efficient heavy-duty engines. By leveraging the benefits of gasoline-like fuels and optimizing combustion strategies, GCI hold the potential to meet stringent emission standards, improve fuel efficiency, and contribute to the sustainability of future transportation solutions.

1.3. Modeling tools

Modeling tools related to TBCs for GCI combustion provide a comprehensive framework for understanding and optimizing the impact of TBCs on engine performance and emissions. To investigate the impact of TBCs on combustion, different simulation tools that link computational fluid dynamics (CFD) and some form of finite element analysis (FEA, a finite difference heat equation solver) to capture the variation in surface temperature from the TBC have been studied. In the pursuit of a higher fidelity understanding of TBC impacts on GCI engines, a multidimensional modeling approach incorporating Conjugate Heat Transfer (CHT) has been advocated [24, 25]. By integrating the solid piston domain with the fluid dynamics of combustion, this methodology enables a distinct analysis of heat transfer across engine components. Validation against experimental data, particularly through thermocouple measurements within piston surfaces, surrounds the credibility of simulation outcomes. Such validated models serve as a robust foundation for exploring the effects of TBCs, offering insights into heat loss mitigation and efficiency enhancements. Moreover, they show the way for innovative engine design strategies that could enhance the thermal insulation properties of TBCs [25].

In recent studies, researchers have been working with advanced modeling tools to better understand how special coatings, known as TBCs, can make engines more efficient. One of the

key tools used in this research is a combination of GT Suite and ANSYS Fluent [26, 27]. GT Suite is a program that simulates the whole engine cycle, showing how the engine runs from start to finish. It helps to predict how changes, like adding a coating, can affect engine performance. ANSYS Fluent, on the other hand, focuses on how fluids and gases move and interact with surfaces, which is crucial for understanding how heat moves through an engine. The researchers used these tools to explore how TBCs change the temperature inside the engine during different parts of the engine cycle, like when fuel is ignited or when exhaust gases are released [28, 29, 30]. They found that the right kind of TBC can significantly reduce the amount of heat lost from the engine, making it up to 1.5% more efficient. This might not sound like much, but it's a big for fuel savings and reducing emissions over time. But it's not just about making the engine more efficient; the coating also needs to be durable. The Johnson-Cook damage model, another sophisticated tool, was used to predict how long these coatings might last. This model looks at how materials behave under different stresses, temperatures, and strains, which is essential for understanding how the TBC will hold up over the life of the engine [31, 32].

All these methods did not have the fidelity to generate reasonable BCs. Moser et al. [33] showed the CFD-FEA framework to predict the temperature swing of TBCs and its impact on heavy-duty diesel engine performance. Motwani et al. [34] adopted Moser's CFD-FEA co-simulation framework to understand the impact of novel TBCs on heat transfer in spark ignition engines. This study showed a 7% reduction in wall heat transfer due to a reduced temperature difference between the piston wall and working gas. In the present work, the same CFD-FEA co-simulation routine was developed used by Moser and Motwani to investigate the effects of TBCs on advanced GCI combustion. This co-simulation methodology was used to estimate the peak surface temperature of the high-performance TBC (up to 1000K), the heat transfer reduction, and

the effect of TBC on combustion and efficiency in GCI. The following section depicts the computational model development on CFD and FEA, followed by the results and discussion of the CFD model validation and FEA heat transfer solutions that contribute to the results of CFD-FEA co-simulation.

1.4. Heat Transfer prediction through TBCs

In GCI combustion, heat transfer prediction through TBCs is crucial for optimizing engine performance and durability. TBCs are applied to engine components to reduce heat transfer, thus maintaining lower temperatures in critical areas such as combustion chambers and exhaust systems. Predicting heat transfer through TBCs involves computational modeling techniques that consider factors like coating material properties, thickness, surface roughness, and operating conditions [26, 27]. These models simulate heat conduction, convection, and radiation processes within the engine to estimate temperature distributions and heat fluxes across TBC-coated surfaces. By accurately predicting heat transfer, engineers can optimize TBC designs to enhance engine efficiency, reduce thermal stresses, and improve overall performance in GCI combustion engines.

Understanding heat transfer through TBCs in GCI is a complex process, pivotal for enhancing engine efficiency and durability. TBCs, essentially sophisticated heat-resistant layers applied to engine components, play a crucial role in managing the engine's thermal environment. They aim to minimize heat loss and protect the engine's structural integrity by maintaining lower temperatures within crucial zones such as the combustion chamber and exhaust systems. The process of predicting heat transfer through these coatings involves advanced computational modeling techniques that account for various parameters including the material properties of the

coatings, their thickness, surface characteristics, and the operational conditions of the engine [30, 31, 32].

In a simulated study designed to investigate the effects of TBCs on GCI combustion, we adopted a computational approach that integrates both CFD and FEA. This hybrid simulation framework enables a comprehensive analysis of heat flow and temperature distribution across the coated engine components under different operating conditions. CFD simulations provide detailed insights into the fluid flow and heat transfer processes within the engine, capturing the complex interactions between the combustion gases and coated surfaces. This includes evaluating how effectively TBCs can reduce heat transfer through conduction, convection, and radiation mechanisms, thereby influencing the thermal load on the engine components. Simultaneously, FEA contributes to understanding the thermal stresses and strains induced by the operational heat loads. It assesses the TBCs' durability by simulating the mechanical responses of coated surfaces to thermal expansions and contractions. This is crucial for ensuring the long-term reliability of TBC applications in GCI, as it helps identify potential failure points and optimize coating materials and thicknesses for better performance.

To validate the accuracy of our simulation, we compared the computational predictions with experimental data, ensuring that our model accurately reflects the real-world behavior of TBCs under GCI combustion conditions. This validation step is critical for confirming the reliability of the simulation results and for making informed decisions regarding the design and application of TBCs in enhancing GCI efficiency. Through this comprehensive modeling approach, we aim to search deeper into the impact of TBCs on the thermal management and overall efficiency of GCI engines. By accurately predicting heat transfer and assessing the thermal durability of TBCs, we

can optimize coating designs to achieve better fuel efficiency, reduce emissions, and extend the lifespan of engine components.

1.5. Objectives of the current study

Most of the current study is related to the temperature-swing behavior of 250-micron thick Gadolinium Zirconate (Gd-Zr) TBCs and its impact on thermal efficiency and heat transfer losses in a light-duty single-cylinder research engine. A coupled CFD-FEA methodology is developed that links a CFD model to FEA model of the piston within which several iterations is performed until a quasi-steady state converged solution was reached. Low-temperature GCI has shown characteristics on ultra-low emissions and high thermal efficiency engine operation. The study aimed to understand the impact of TBCs on engine cycles, identify areas of high temperature and heat fluxes on the coating, and evaluate any resulting improvements in engine efficiency. The co-simulation framework is used to analyze thermal boundary conditions and predict efficiency gains. Finally, the study aimed to compare the predicted efficiency improvements from the modeling approach with experimental testing results to validate the effectiveness of TBCs in enhancing engine performance.

The objectives of the study are summarized below:

- To develop and validate a co-simulation framework that integrates CFD and FEA for studying the impact of TBCs on GCI combustion.
- To investigate the effect of Gadolinium Zirconate (Gd-Zr) TBC on the temperature behavior of engine components, specifically focusing on the piston surface temperature swings during engine cycles.
- To assess the influence of TBCs on heat transfer losses and thermal efficiency within the GCI combustion environment under various operational pressures.

- To quantify the improvements in thermal efficiency due to TBC application through computational predictions and compare these with experimental results to evaluate the fidelity of the models.
- To identify and analyze the discrepancies between simulated predictions and actual experimental outcomes to enhance the understanding of TBC behavior in real-world engine conditions.
- To provide a foundation for future research directions, including the refinement of simulation models, exploration of different TBC materials, and assessment of TBCs in practical engine applications for sustainability and performance enhancement.

CHAPTER TWO

MODELING METHODOLOGY

This chapter describes the methodology for modeling the phenomena which includes CFD and FEA model development along with their detailed specifications. Different factors like initial conditions, boundary conditions, grid sizes, geometry, etc. are discussed.

2.1. 3D CFD Computational Model

A 3D CFD model was created using CONVERGE 3-D CFD software [35]. The model geometry was developed from Computer-Aided Design (CAD) models of relevant production engine parts provided by Aramco Services Company (ASC) in support of this study. Figure 3 shows the computational model developed for single cylinder, experimental engine. The simulation featured an injector positioned at the center, modeled accurately within CONVERGE Studio. The model's mesh began with a uniform 3mm grid throughout its structure, which was subsequently refined to 0.75mm in the combustion chamber, reduced to 0.3mm around the intake and exhaust valves to better capture fluid movement during valve operations, tightened to 0.18mm near the injector spray areas during fuel injection, and adjusted to 1mm around the piston crown. This refinement aimed to improve the simulation's resolution of near-wall effects, using a fixed embedding approach for mesh enhancement.

The simulation modeled the dynamic behavior of intake and exhaust valves through intake and exhaust valve profiles. These files defined the timing, lift, and duration of valve openings, which are critical for capturing the engine's breathing dynamics. Accurate representation of valve motion is crucial for predicting the flow of mixtures into and out of the combustion chamber and hence for the overall performance of the engine. The use of an adaptive mesh refinement strategy

played a pivotal role in enhancing the simulation's accuracy and efficiency. This technique allowed for dynamic adjustment of the mesh resolution in regions of high gradient, such as in the vicinity of the flame front or near solid boundaries.

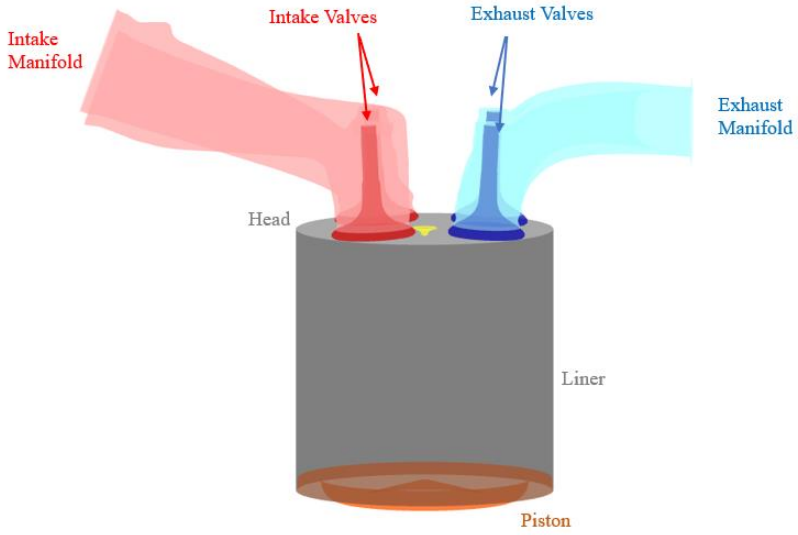

Figure 3: Computational model developed for single cylinder, experimental engine

Table 1 shows the engine specifications of single cylinder, experimental GDI engine.

Table 1: Engine specifications of single cylinder, experimental GDI engine

Bore	82mm
Stroke	80.1mm
Connecting Rod Length	152.4mm
Geometric Compression Ratio	15.6:1
Intake Valve Opening/ Closing	-360/-153 CAD aTDC
Exhaust Valve Opening/ Closing	127/358 CAD aTDC
Engine speed	1500 rpm

The RNG k-ε was used which is a way to study turbulence in fluids, like in engines. It helps us understand how the fluid moves and mixes. It offers enhanced performance in capturing the impact of swirls, rapid strain, and streamlined curvature on turbulence, making it suitable for complex flows [35]. Then, dynamic drop drag model was used which helps to figure out how the droplets interact with the fluid around them. Frossling correlation was also used to see how the droplets turn into vapor [36, 37].

The Kelvin-Helmholtz and Rayleigh-Taylor (KH-RT) hybrid model was used to simulate the breakup of liquid sprays. This model combines the strengths of two fundamental theories of fluid instability to predict the behavior of liquid jets more accurately as they break up into droplets upon entering a gaseous medium, a critical process in the atomization and mixing of fuel. The

Kelvin-Helmholtz (KH) model primarily addresses the shear-induced breakup of the liquid jet due to the velocity difference between the liquid and the surrounding gas. The Rayleigh-Taylor (RT) model, on the other hand, focuses on the breakup due to density differences between the liquid and the gas, particularly effective under conditions of acceleration or deceleration [38-41]. This aspect of the model captures how denser liquid parcels, under the influence of body forces, penetrate the lighter gas, leading to the formation of ligaments and smaller droplets. By integrating these two mechanisms, the KH-RT hybrid model provides a comprehensive framework for simulating spray breakup. It effectively accounts for both the aerodynamic shear forces and the body forces acting on the liquid jet, leading to more accurate predictions of droplet size distribution, spray penetration, and spray angle [41]. Table 2 shows the specifications of the injector used. The wall heat transfer model and spray wall interaction model were developed using O'Rourke and Amsden [38].

Table 2: Injector specifications

No. of nozzle holes	8
Nozzle diameter [µm]	110
Spray included Angle [°]	150
Spray Cone Angle [°]	17
Nozzle Discharge Coefficient [-]	0.79

For the chemistry part, SAGE model was used which is a detailed chemical kinetics solver that predicts combustion by solving transport equations for mass, momentum, and energy, coupled with chemical reaction rates developed by Senecal et al. [42]. It excels in simulating complex combustion processes, including flame propagation and pollutant formation, by directly integrating detailed reaction mechanisms for a wide range of fuels. We model the reactions of

gasoline using a mix of 87% iso-octane and 13% n-heptane. This helps us predict the emissions except for soot. For soot, we use a separate model using the Hiroyasu-NSC soot model to see how it forms and gets burned up inside the engine [43, 44].

2.2. 3D FEA Model Framework

The FEA Model was developed using ABAQUS 2020 [45] using the CAD model of the piston. The FEA modeling primarily involves simulating the heat transfer dynamics between the piston and the engine's combustion chamber. This method aims to understand how the TBC layer influences the piston's temperature profiles and, by extension, the engine's overall thermal efficiency and performance. The mesh size for the base metal piston was 5mm whereas the piston crown has in the order of 1 mm. Figure 4 shows the geometry of piston with TBC layer coated on top. The TBC shell elements were on the order of 1mm with DS3/DS4 [46] offset shell elements added to the piston crown, with an assumed perfect heat conduction constraint between the piston crown surface and the underside of the TBC. The shell elements were solved using Simpson's integration routine with 19 integration points for each element within the TBC shell [45, 46].

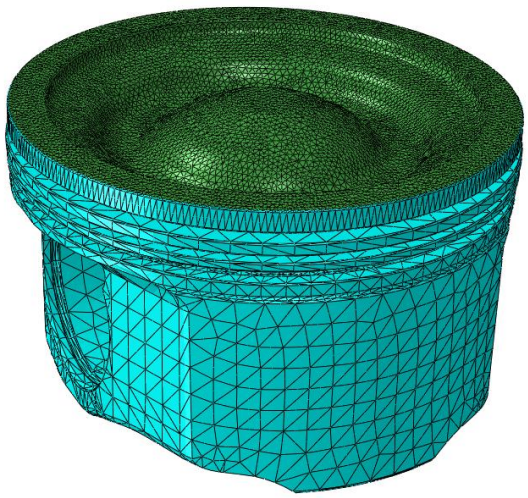

Figure 4: Geometry of piston with TBC layer coated on top (green)

Table 3 shows the material properties of the piston and TBC material.

Table 3: Piston and TBC material properties

Components	**Piston**	**TBC**
Density	5000 kg/m^3	5850 kg/m^3
Specific heat capacity	600 J/kg K	430 J/kg K
Thermal conductivity	42.5 W/m-K	0.74 W/m-K

The piston geometry, including the TBC layer, is created based on CAD models. The TBC layer is typically modeled as a shell layer on the piston surface to accurately capture its thermal properties and effects. This approach ensures precise thermal analysis of TBCs with reduced simulation time and resource usage, which is less feasible with solid layer modeling for thin coatings. The entire geometry is then discretized into a finite element mesh, where smaller elements are used in regions of high thermal gradient to ensure accurate results. Thermal properties (e.g., thermal conductivity, specific heat capacity, and density) of both the piston material and the TBC are defined within the FEA model. These properties are crucial for accurately simulating heat conduction through the piston and the TBC layer. The thermal boundary conditions are applied based on the simulated combustion heat flux obtained from CFD simulations. This includes spatially resolved temperatures and heat transfer coefficients on the piston surface facing the combustion chamber. For the piston backside, conditions mimic the cooling effects and thermal interactions with engine oil and other components [47]. The FEA simulation is run as a transient

analysis to capture the dynamic changes in temperature across the engine cycle. This involves solving the heat transfer equations over time, considering the applied boundary conditions and the material properties of the piston and TBC. FEA is part of a co-simulation routine with CFD to refine the boundary conditions iteratively. After an initial FEA run, the piston temperature data may be fed back into a CFD model to update the combustion and heat transfer simulations. This process can repeat until a consistent solution is achieved, highlighting the TBC's impact on reducing heat transfer through the piston.

The piston underside consists of the piston top land, middle land, oil land, ring grooves, skirts, skirt underside, crown underside, piston pin holes, and piston underside. The temperature and convective HTC boundary conditions for the underside of the crown and skirts were calculated from the oil temperature and engine speed based on the literature [47]. Table 4 shows the values for temperature and heat transfer coefficient of piston FEA backside boundary conditions. Similarly, the heat transfer coefficients were calculated from the ratio of the thermal conductivity of gas to the clearance between the piston and the liner [48]. The initial conditions for FEA was setup in such a way that it reduces the number of cycles required to reach quasi-steady state. When steady state is achieved, transient analysis was done using the steady state output as initialization. It was performed for three cycles such that it achieves quasi-steady solution where the change in piston surface temperature was less than 2K. Therefore, the average near-wall gas temperatures and heat transfer coefficients for each cycle can be used as initial conditions. This is calculated using equations (i) and (ii):

$$\overline{T_{gas}} = \frac{\sum_i^t h_i . T_{g_i} \, \Delta t}{\sum_i^t h_i . \Delta t} \qquad \text{(i)}$$

$$\bar{h} = \frac{1}{t} \sum_{i}^{t} h_i . \Delta t \qquad \text{(ii)}$$

In the above equations, 'h_i' and 'Tg_i' are the instantaneous heat transfer coefficient and fluid temperature for each point at time interval of (Δt), where 't' is in crank angle degrees.

Table 4: Piston FEA backside boundary conditions

Surfaces	**Heat Transfer Coefficient (W/m^2K)**	**Temperature (K)**
Top Land	138.23	522
Middle Land	126.85	509
Oil Land	126.85	487
Piston Pin	1000	363
Crown Underside	608	363
Skirt	75	363
Skirt Underside	162.13	363
Piston Underside	162.13	363
Ring Grooves	368.18	522
Piston top	CFD combustion output	

CHAPTER THREE

RESULTS AND DISCUSSIONS

3.1. 3D Computational Fluid Dynamics

The CAD parts of engine components were provided by Aramco Services Company (ASC) in support of this research work. At first, the metal baseline pistons were simulated and validated against the experimental data under 6-bar, 10-bar, and 15-bar operating conditions. The motoring data was validated followed by the firing data. For metal baseline, fixed embedding was not imposed on the piston surface. For coated case, a fixed embedding layer of about 1mm was imposed on the piston top surface to mimic the coating. Figure 5 shows the model validations for 6-bar operating conditions. The simulation has sufficient agreement with the experimental data to consider the model validated.

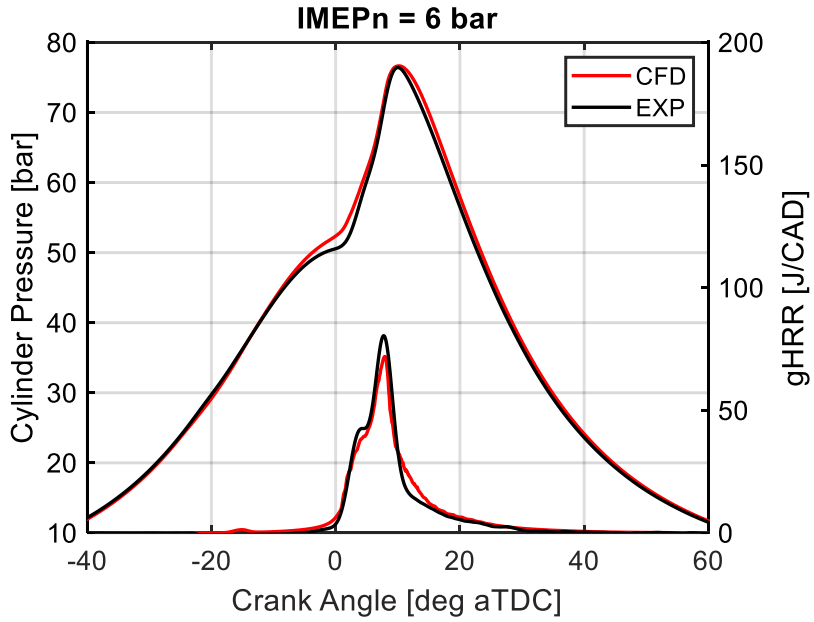

Figure 5: Cylinder pressure vs Gross Heat Release Rate (GHRR) for CFD (red) and Experiment (black) at 6 bar conditions

The CFD simulation (red line) closely follows the experimental data (black line), indicating that at a lower pressure level, the CFD model effectively captures the pressure dynamics within the engine cylinder. This close match suggests that for this relatively low-pressure condition, the simulation can accurately reflect the behavior of the TBC-coated piston, providing insights into how the coating influences engine performance.

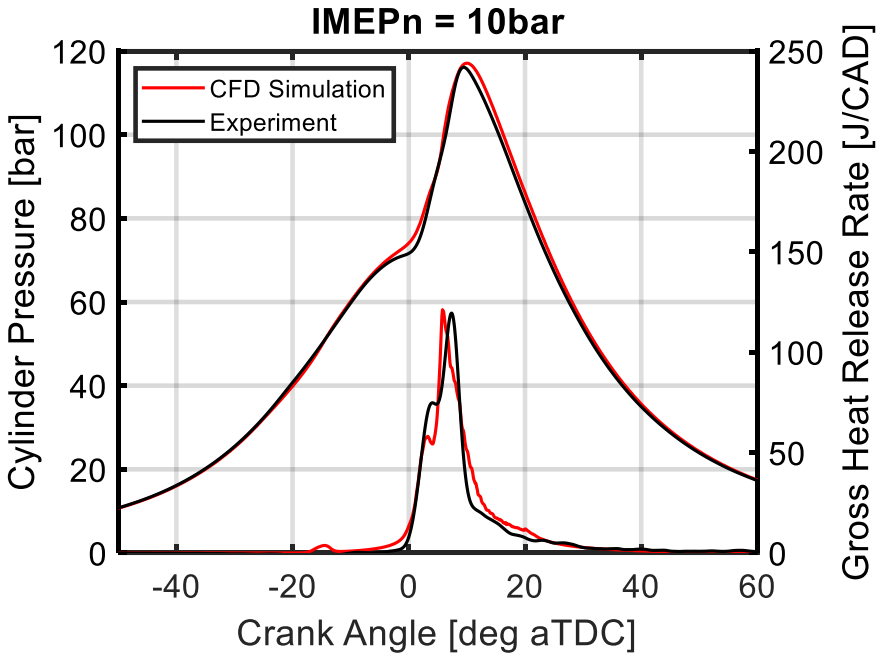

Figure 6: Cylinder pressure vs Gross Heat Release Rate (GHRR) for CFD (red) and Experiment (black) at 10 bar conditions

Figure 6 shows the model validation at 10-bar condition. The graph still displays a good correlation between the CFD simulation and the experimental data, but with slightly more deviation than the 6-bar case. This could be due to the higher pressure in the combustion process, which the model still manages to capture reasonably well.

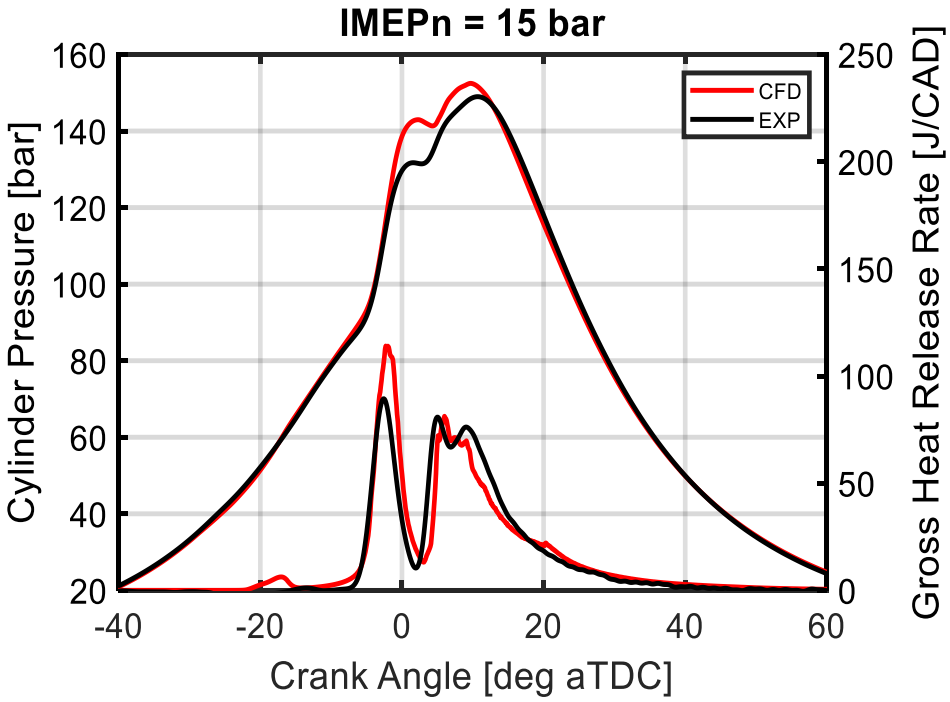

Figure 7: Cylinder pressure vs Gross Heat Release Rate (GHRR) for CFD (red) and Experiment (black) at 15 bar conditions

Figure 7 shows the model validation for the 15-bar condition. The graph shows the highest operating pressure and indicates a difficult environment for the CFD simulation to replicate. Despite this, the CFD results align well with the experimental data, demonstrating the model's capability to simulate the pressures and temperatures associated with the TBC-coated piston's operation even at high pressures.

Additionally, a split fraction sweep was performed for the validation of CFD and the experimental traces. The experimental split fraction was 43% for the pilot injection and 57% for the main injection. The CFD model previously validated has the split fraction the same as the experiment. The sweeps were performed by increasing the main injection split fraction from 57% to 67%, from where 62% of the main injection and 38% of the pilot injection seem to agree reasonably well with the experiment. Figure 8 shows the cylinder pressure versus gross heat release rate for different

split fractions from CFD along with the experiment at 15 bar conditions. A slight change in intake temperature was also performed but there were no reasonable changes observed. The lack of changes could be due to the negative temperature coefficient (NTC) phenomenon. In the NTC region, the increasing temperature doesn't significantly alter the ignition delay or the rate of combustion. In other words, the combustion process may not accelerate as expected even when the intake temperature is adjusted. On top of that, due to differences in the chemical kinetics mechanism used in the model and the actual kinetics, slight differences were still observed in the heat release process, but overall the split fraction of 38/62 agrees with the experiment.

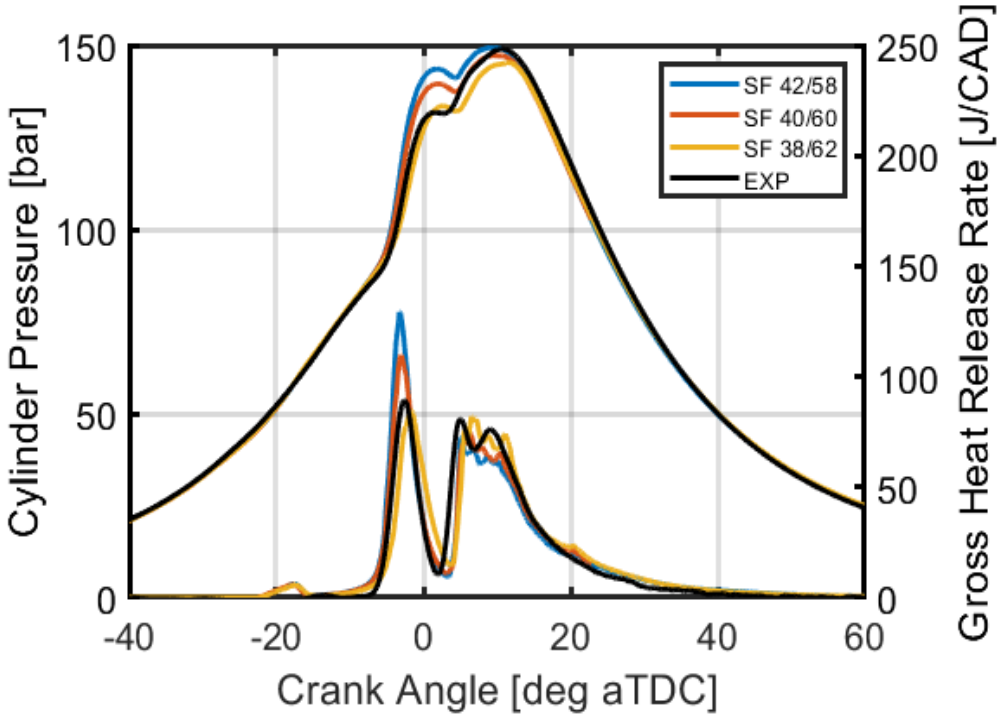

Figure 8: Cylinder pressure vs Gross Heat Release Rate (GHRR) for different split fractions (SF) with the experimental trace (black) at 15 bar conditions

3.2. 3D Finite Element Analysis

The boundary conditions from 3D CFD output are imposed to FEA model of the piston. At first, the metal baseline is simulated. Figure 9 shows the coated piston surface temperature and nodal temperatures for 6 bar conditions.

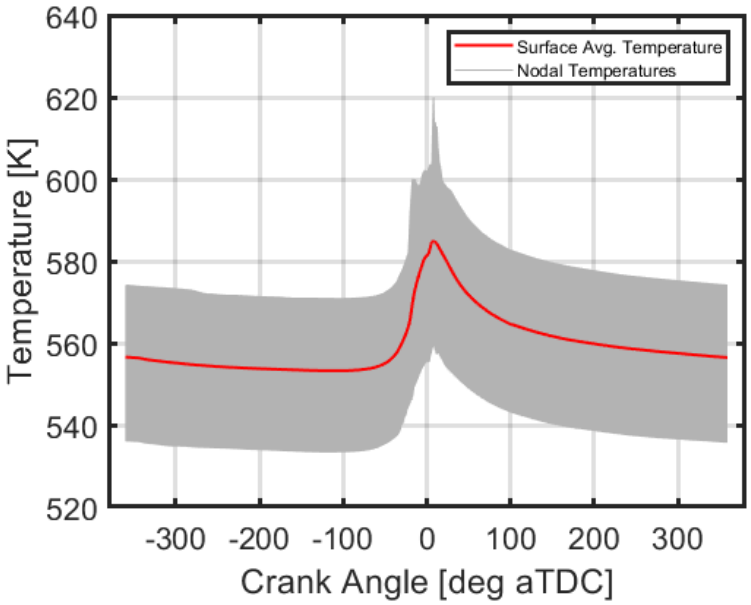

Figure 9: Surface average temperature (red) and Nodal Temperatures (grey) variation for TBC coated piston at 6 bar conditions

In case of the 6-bar condition, the temperature variation observed is relatively moderate, with a swing of approximately 40K around the top dead center (TDC). This suggests that under lower load conditions, the TBC-coated piston is subjected to less intense combustion temperatures. The relatively stable temperature indicates that the TBC material is effectively insulating the piston surface and that the thermal load is within the material's capacity to absorb and dissipate heat efficiently. The reduced temperature swing at 6 bar can be attributed to a lower rate of heat generation in the combustion chamber and the higher effectiveness of heat transfer mechanisms such as conduction and convection at lower gas densities. Figure 9 shows the surface average

temperature and nodal temperatures at 10-bar conditions. There is a significant increase in the temperature swing, reaching around 100K.

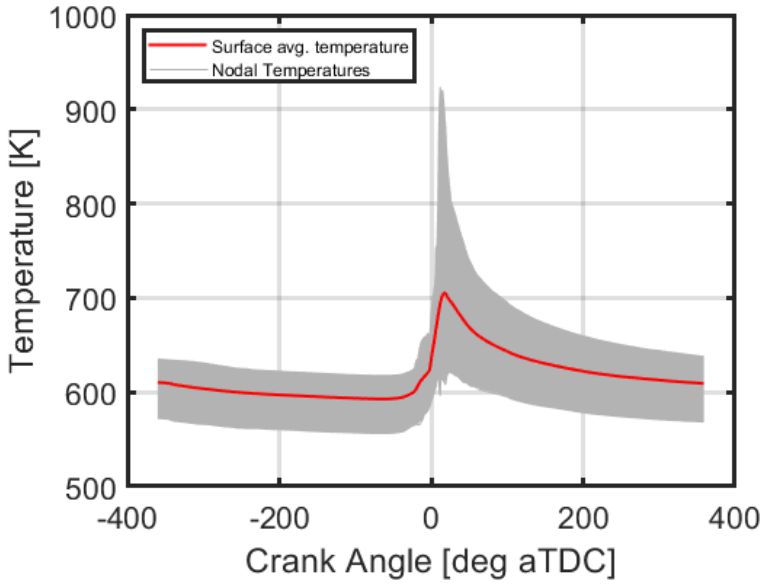

Figure 10: Surface average temperature (red) and Nodal Temperatures (grey) variation for TBC coated piston at 10 bar conditions

The larger temperature variation reflects a more vigorous combustion process, which in turn generates more heat. At this intermediate pressure condition, the TBC is still performing its insulative role, but the increased heat flux from the combustion gases to the piston surface results in higher surface temperatures. The spike in temperature near TDC is indicative of the peak combustion event where the highest amount of energy is being released. The 10-bar condition represents a transition from moderate to more demanding thermal loads on the TBC material. Figure 10 shows surface average temperature and nodal temperatures for 15- bar conditions. This further intensifies the temperature swing, also exhibiting a variation of about 150K but at a higher overall temperature level.

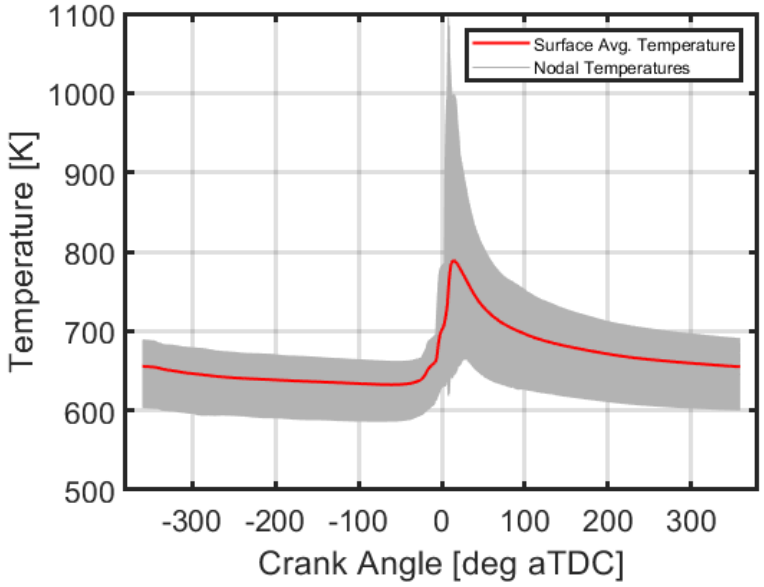

Figure 11: Surface average temperature (red) and Nodal Temperatures (grey) variation for TBC coated piston at 15 bar conditions

This increased temperature response is consistent with an even more intense combustion environment, expected at higher engine loads. The thermal spike near TDC is more pronounced, which implies that the TBC has reached a state of higher thermal saturation, and there is an increased challenge in dissipating the heat quickly. It also indicates that the TBC's ability to protect the piston material might be approaching its limits, as the extreme temperatures are closer to the degradation point of TBC materials.

3.3. 3D CFD-FEA Co-simulation

The 3D CFD model was first ran with constant piston wall temperature of 450K which is the CFD Baseline case. After running the first FEA iteration with piston thermal boundary

conditions from CFD, transient wall temperature profile was generated from FEA which was used for the next iteration of CFD-FEA Co-simulation.

The figures below show plots of cylinder pressure versus gross heat release rate for different CFD iterations during co-simulation at 6 bar, 10 bar, and 15 bar conditions. These plots are essential for validating the CFD model's ability to simulate the real-world behaviors observed in engine testing (EXP). The data from these simulations helps in understanding the combustion dynamics within the engine cylinder for each operating condition. Figure 11 shows the cylinder pressure vs Gross Heat Release Rate from CFD output during the co-simulation iterations at 6-bar conditions.

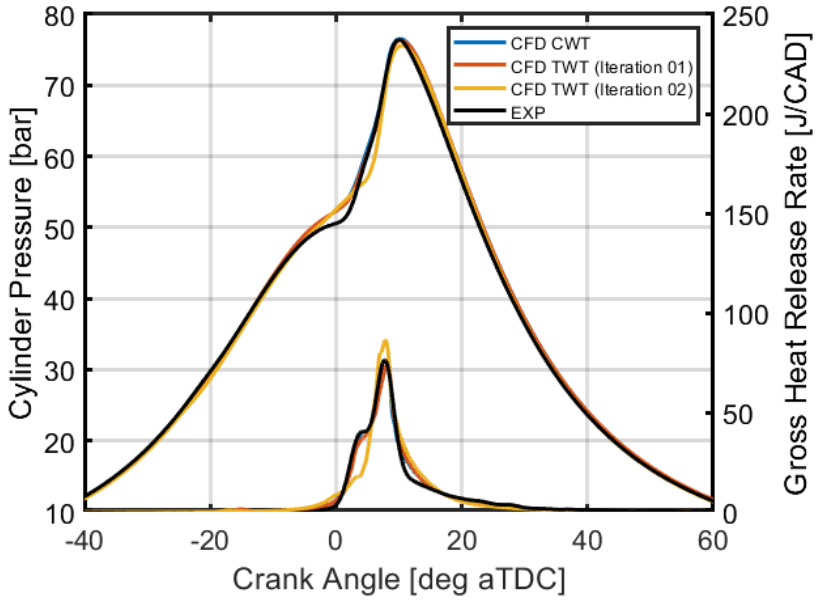

Figure 12: Cylinder pressure vs Gross Heat Release Rate from CFD output during the co-simulation iterations at 6 bar conditions

The 6-bar condition shows two CFD iterations with transient wall temperatures and their comparison to experimental data. The first iteration of the CFD model closely follows the experimental pressure curve but deviates slightly in the gross heat release rate. In the second

iteration, the agreement improves, indicating that the model's predictive capability is enhanced through iterative refinement. The heat release rate in both iterations closely follows the experimental data with minor discrepancies, suggesting that the combustion timing and the rate of heat release are accurately captured after the second iteration. This level of validation shows that the model can predict the pressure and heat release characteristics at this lower operating pressure with high fidelity. Figure 12 shows cylinder pressure vs Gross Heat Release Rate from CFD output during the co-simulation iterations at 10-bar conditions. It includes two CFD iterations and their comparison to the experimental data.

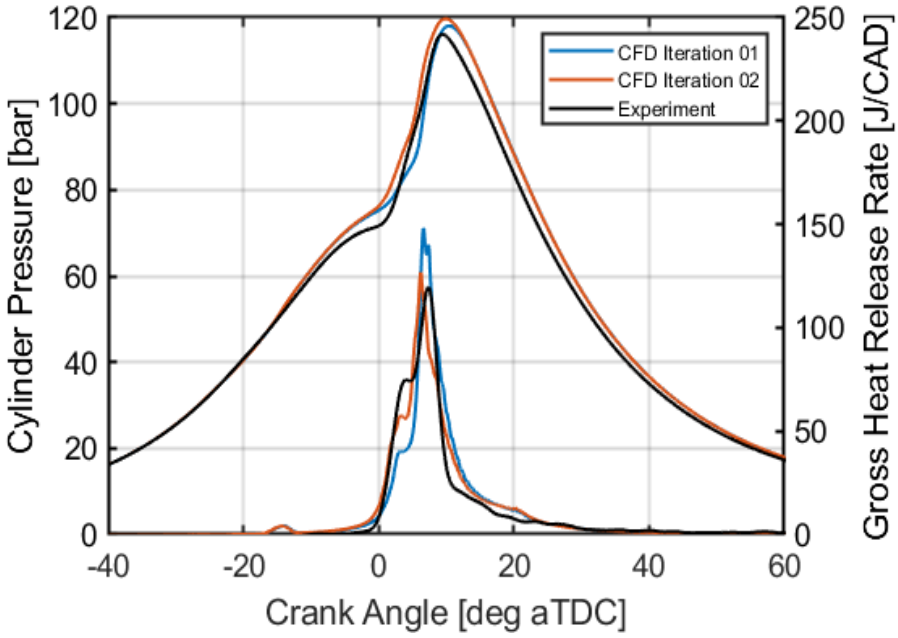

Figure 13: Cylinder pressure vs Gross Heat Release Rate from CFD output during the co-simulation iterations at 10 bar conditions

The initial CFD iteration reveals a discrepancy in both the cylinder pressure and heat release rate when compared to the experimental data. However, the second iteration shows a better alignment with the experimental curves, especially in the peak heat release rate, although slight variations still exist in the tail of the combustion event. The differences between iterations indicate that adjustments to the model, possibly in fuel injection timing, mixture formation, or combustion

kinetics, are improving its accuracy. The model is adjusting to better capture the more complex combustion phenomena occurring at this increased pressure. Figure 13 shows model validations for different co-simulation iterations at 15-bar conditions. The pressure and gross heat release rate for second iteration of CFD is not matched correctly.

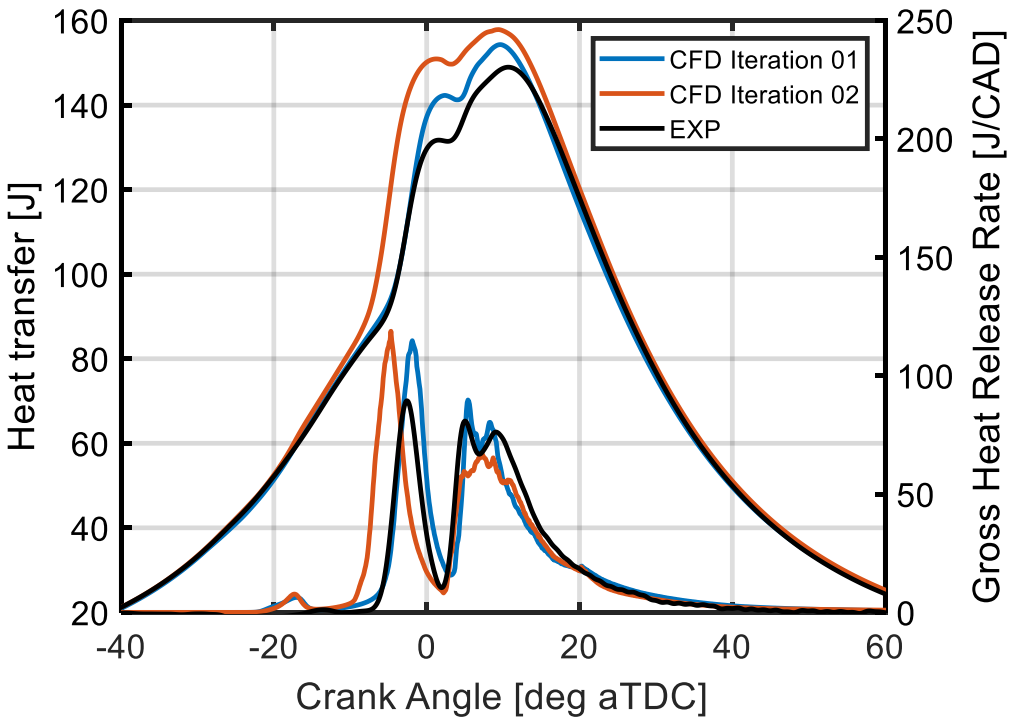

Figure 14: Cylinder pressure vs Gross Heat Release Rate from CFD output during the co-simulation iterations at 15 bar conditions

Due to more computational time required and less time available, were not able to match it perfectly, but EGR sweeps could be performed in future study to match it with the experimental traces. The differences between CFD iterations and experimental data are more pronounced for 15 bar conditions. This is likely due to the higher pressures and temperatures, which can increase any small inaccuracies in the model. The first iteration significantly deviates from the experimental data in predicting both cylinder pressure and heat release rate. However, the second iteration

corrects much of this discrepancy, particularly in the gross heat release rate following the combustion event. The remaining differences may originate from the challenges of modeling the complex interactions of spray patterns, turbulence, and heat transfer at higher operating pressures.

During the co-simulation routine, the heat transfer data from CONVERGE, which shows how heat moves on the piston surface over time, was sorted using a MATLAB script. Figure 15 shows 3D CFD-FEA Co-simulation Framework developed for the current study. This script organized the data based on where it was on the piston and what the temperature was. Then, a new time step was created using a Python script in Abaqus, a software used for simulating engineering problems. This new time step used the heat transfer data to make sure the heat flow was accurate. After the simulation, the results, which showed the temperature of the piston surface at different times and places, were saved in a text file. This file was then used in the next iteration of the simulation in CONVERGE.

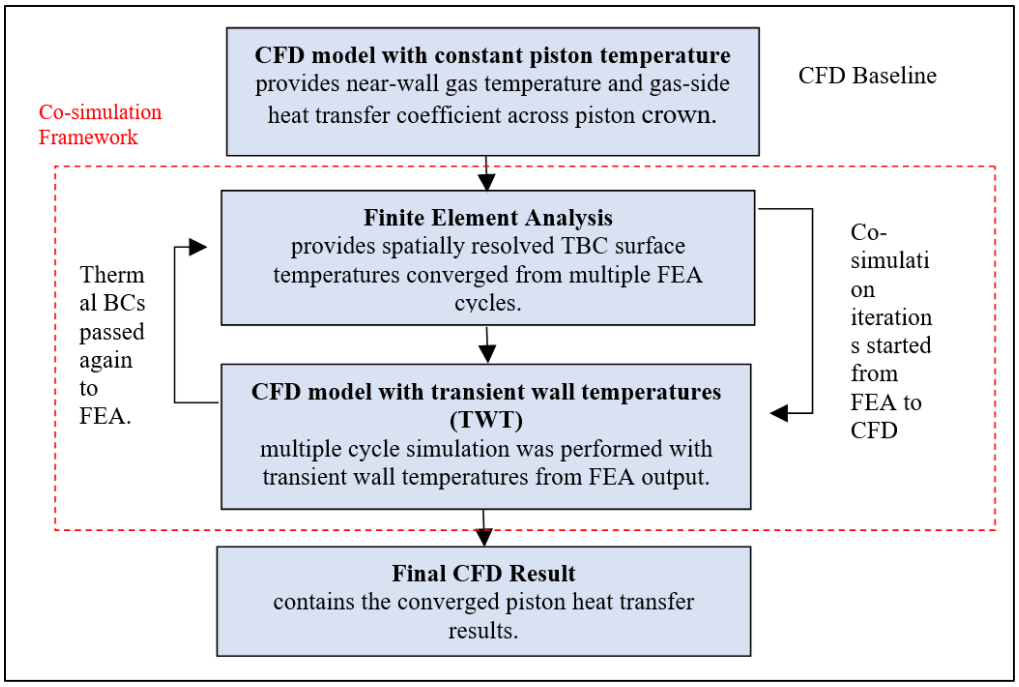

Figure 15: 3D CFD-FEA Co-simulation Framework.

The co-simulation was performed for a 250-micron thick TBC layer, where the temperature swing phenomenon depends on the difference between gas and the wall that reduces heat transfer through the piston. Since the change in cycle averaged uncoated piston temperature was less than 2K, a quasi-steady solution can be assumed. Figure 16 shows the surface average temperature variations during an engine cycle for the uncoated and coated pistons along with constant wall temperatures used as initialization for metal and TBC cases.

The co-simulation begins with a CFD model assuming a constant piston wall temperature. The baseline temperature was set at 450K. This initial simulation provides a preliminary set of thermal boundary conditions that are then fed into an FEA model. The FEA model, in turn, simulates the transient thermal behavior of the piston material, considering the TBC's thermal properties. After the first FEA iteration, the resulting transient wall temperature profile is then reintroduced into the CFD model. This marks the beginning of the next iteration of the CFD-FEA co-simulation. The process is iterative because it continually refines the temperature profile by accounting for the dynamic interaction between the heat transfer at the piston surface and the temperature-induced material responses.

The first three figures represent the co-simulation validation step, displaying the pressure vs. heat release rate for 6 bar, 10 bar, and 15 bar conditions of a coated piston. These plots are crucial as they compare the simulated data against experimental data (EXP) to validate the model's accuracy. Each curve in these plots corresponds to different iterations within the co-simulation process, showing how the model predictions evolve with each successive iteration. The final plot illustrates the surface average temperature for various operating conditions and compares them between coated and uncoated pistons. This plot is vital for assessing the effectiveness of the TBC in maintaining acceptable piston temperatures under different engine loads. The TBC layer's

primary function is to insulate the piston from the high temperatures generated during combustion, and this plot effectively shows the TBC's impact on temperature control. It reveals that the temperature swings for the TBC-coated pistons are within a range that ensures both thermal protection and efficient engine operation. The comparison with uncoated pistons demonstrates the TBC's significant role in reducing the thermal load on the piston.

This co-simulation framework, with its detailed data management using MATLAB and Python scripts, provides a robust method for predicting the thermal performance of TBC-coated pistons. By utilizing iterative CFD-FEA cycles, the model can predict how the TBC layer affects piston temperatures under various loads and conditions. The resulting temperature profiles not only inform the design and application of TBCs but also contribute to the optimization of engine performance and longevity. The quasi-steady solution assumption, based on minimal temperature variation in the uncoated piston, further refines the simulation process by simplifying the initial condition setup.

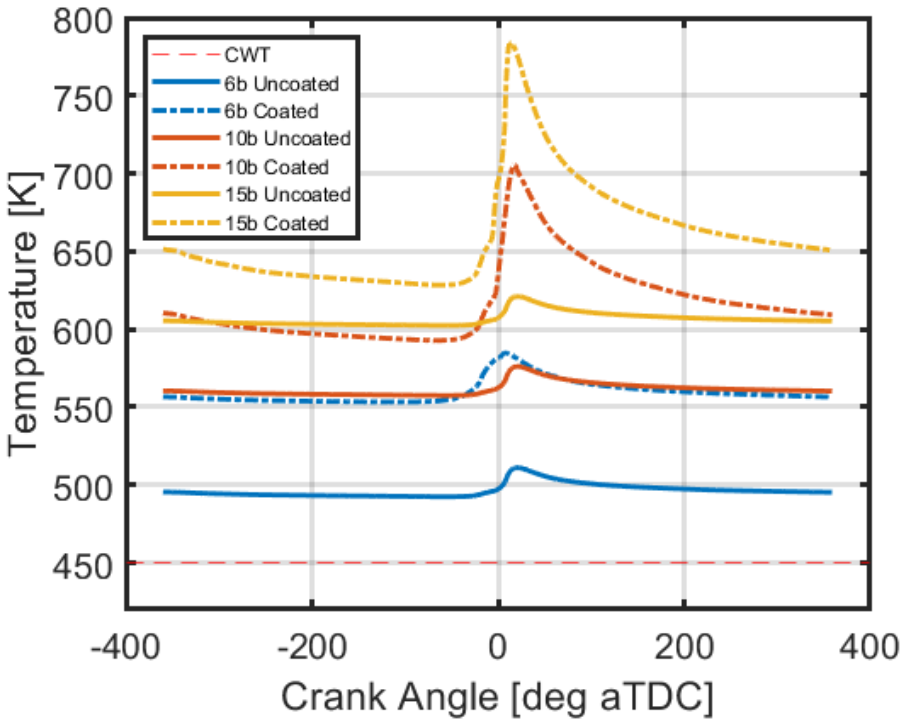

Figure 16: Comparison of piston surface averaged temperature for uncoated (solid) and coated (dashed) cases for the final iteration of FEA with transient wall temperatures along with constant wall temperature (red-dashed)

The plot illustrates the surface temperature variations of pistons with and without TBCs under different operating pressures (6 bar, 10 bar, and 15 bar). This graphical representation captures the influence of TBCs on piston temperature dynamics during an engine cycle.

At the lowest operating condition of 6 bar, the plot reveals that both coated and uncoated pistons experience similar temperature profiles during the initial part of the engine cycle. As the cycle progresses towards and past top dead center, where combustion occurs, the surface temperatures rise sharply. The coated piston shows a higher peak temperature compared to the uncoated piston. This indicates that the TBC is somewhat effective at insulating the piston's surface, reducing the extremity of the temperature spike during combustion. After the peak, the

temperatures for both pistons descend, but the coated piston maintains a higher temperature than the uncoated one for a longer duration, suggesting that the TBC retains heat more effectively.

As load condition increases to 10 bar, the differences in temperature profiles become more pronounced. The uncoated piston's temperature rises more steeply and peaks higher than at 6 bar, illustrating the increased thermal load at this higher operating pressure. The coated piston, however, shows a moderated temperature rise, with the peak temperature being significantly lower than that of the uncoated piston. This suggests that the TBC's thermal insulation properties are more effective at this mid-range pressure. The temperature of the coated piston post-combustion remains higher compared to the uncoated one, which could indicate better heat retention that could be beneficial for the expansion stroke in the engine cycle.

At the highest load of 15 bar, the effect of the TBC is most evident. Here, the temperature differences between coated and uncoated pistons are distinct. The uncoated piston reaches the highest peak temperature among all conditions, indicative of the intense heat generated during high-pressure combustion. The descent in temperature after the peak is more gradual for the coated piston compared to the uncoated one, suggesting a sustained retention of heat, which may contribute positively to the efficiency of the combustion process by reducing the rate of heat loss.

Overall, the plot demonstrates the effectiveness of TBCs in extreme surface temperatures on pistons within a GCI engine. The surface average temperature swing for TBC for 6-bar was only 30K as compared to 10-bar which was about 100K and for 15-bar about 150K. This trend can be attributed to the fact that as the pressure inside the combustion chamber increases, so does the energy release from the combustion process, which leads to greater thermal loads on the piston surface. The TBC, acting as a thermal insulator, will exhibit larger temperature swings at higher pressures because it is more challenging to mitigate the extreme temperature variations during the

combustion cycle. At lower pressures, the energy release from the combustion process, resulting in a smaller temperature differential between the peak and the baseline, thus a lower temperature swing in the TBC. These properties of TBCs can be instrumental in enhancing GCI engine efficiency, especially under high-load conditions where optimal thermal management is of prime importance. Figure 16 shows near-wall gas temperature and heat flux for three different crank angles at 6-bar conditions. The left diagram shows the temperature of the gases close to the cylinder walls. The color spectrum from red to blue represents high to low temperatures, respectively.

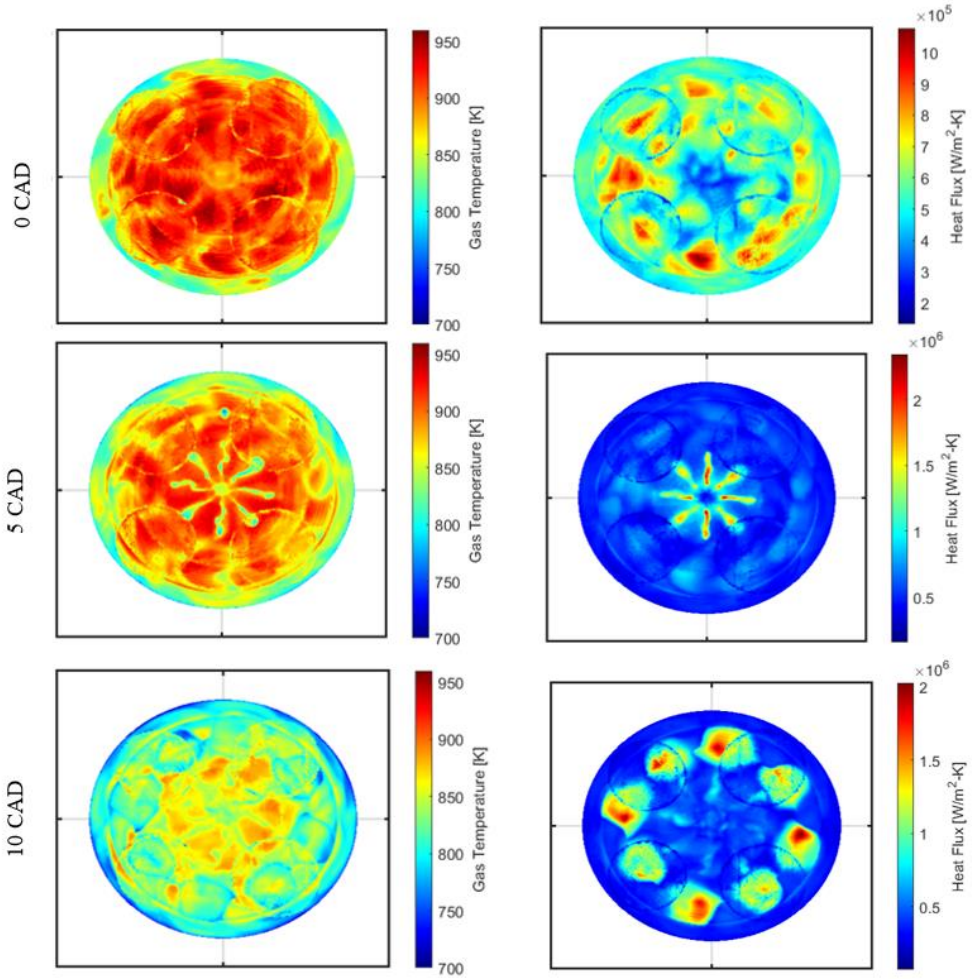

Figure 17: Near-wall gas temperature (left) and heat flux (right) at 0 CAD, 5 CAD and 10 CAD aTDC for 6 bar conditions

At 0 CAD, we see a vibrant red throughout, indicating high temperatures evenly spread out. As the piston moves downwards (5 CAD and then 10 CAD), the high-temperature areas become more concentrated and less widespread, suggesting the combustion gases are cooling down or moving away from the walls. The right column demonstrates the heat flux, which is how much heat is being transferred from the hot gases to the cylinder walls, depicted in a color scale where red signifies more heat transfer and blue indicates less. Initially, at 0 CAD, there are several patches where the heat transfer is particularly high (shown in red). Moving to 5 CAD and then to 10 CAD, the pattern changes and overall heat transfer reduces, as indicated by the increasing blue

areas. Figure 17 shows near-wall gas temperature and heat flux for three different crank angles at 10-bar conditions. The images on the left illustrate the temperatures of gases close to the cylinder wall at three different times.

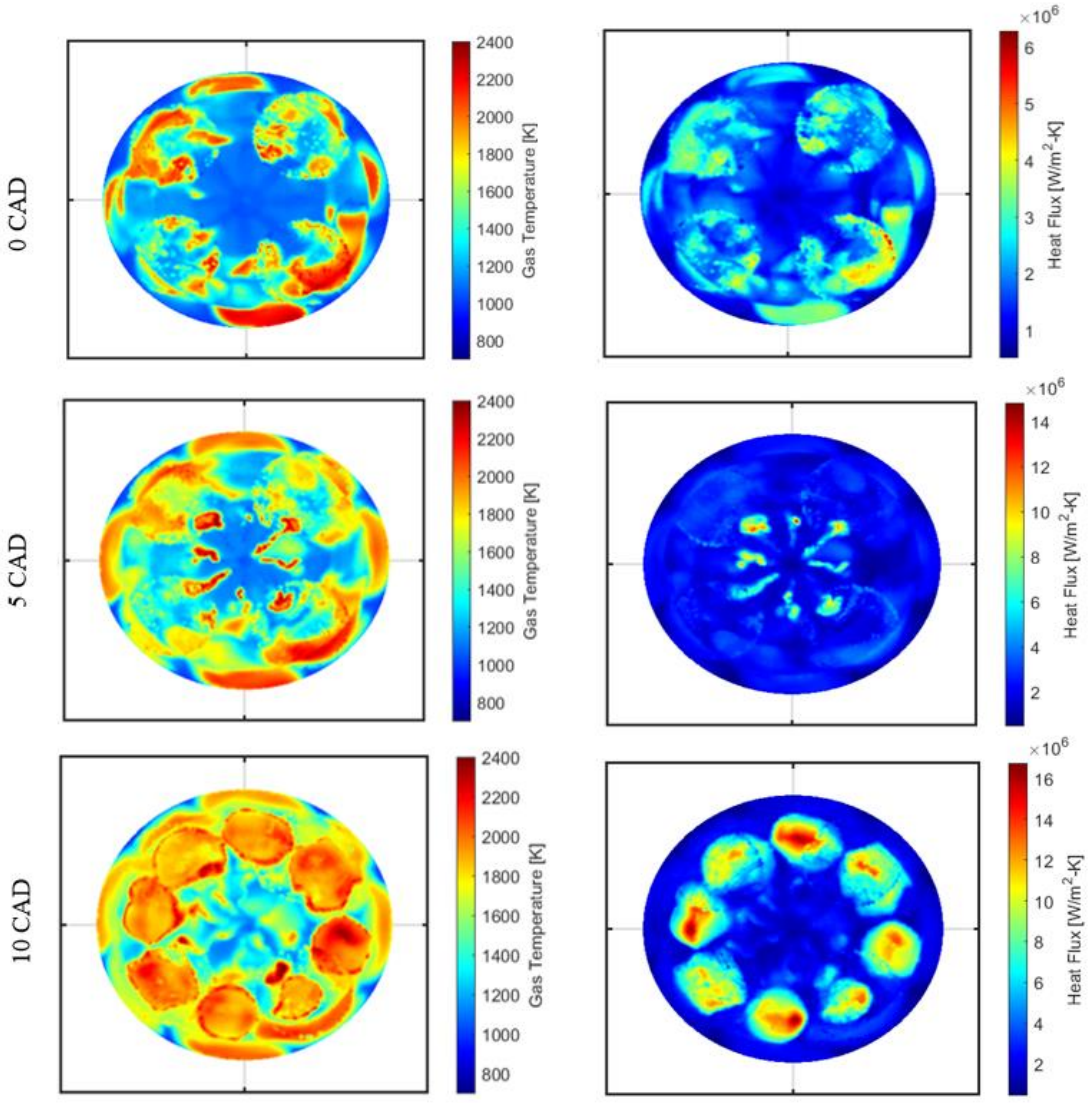

Figure 18: Near-wall gas temperature (left) and heat flux (right) at 0 CAD, 5 CAD and 10 CAD aTDC for 10 bar conditions

The blue areas are cooler and the red areas are hotter. At 0 CAD, there are both hot and cool spots inside the cylinder. As time progresses (5 CAD and then 10 CAD), the red hot spots increase in size and intensity, showing that the gases in these areas are getting hotter as the piston

moves downwards after TDC. Similar to the temperature images, the colors for heat flux range from blue to red, indicating low to high heat flux, respectively. At 0 CAD, the heat transfer is more concentrated in certain areas, as indicated by the patches of red. As the piston descends (5 CAD to 10 CAD), the heat flux pattern changes significantly. At 10 CAD, the heat flux is generally higher across most of the cylinder wall, indicating that more heat is being transferred to the wall at this point in the cycle compared to the moment of TDC. Figure 19 shows near-wall gas temperature and heat flux for three different crank angles at 15-bar conditions. For each of these three times, the colors range from blue to red, with red indicating hotter areas and blue indicating cooler areas.

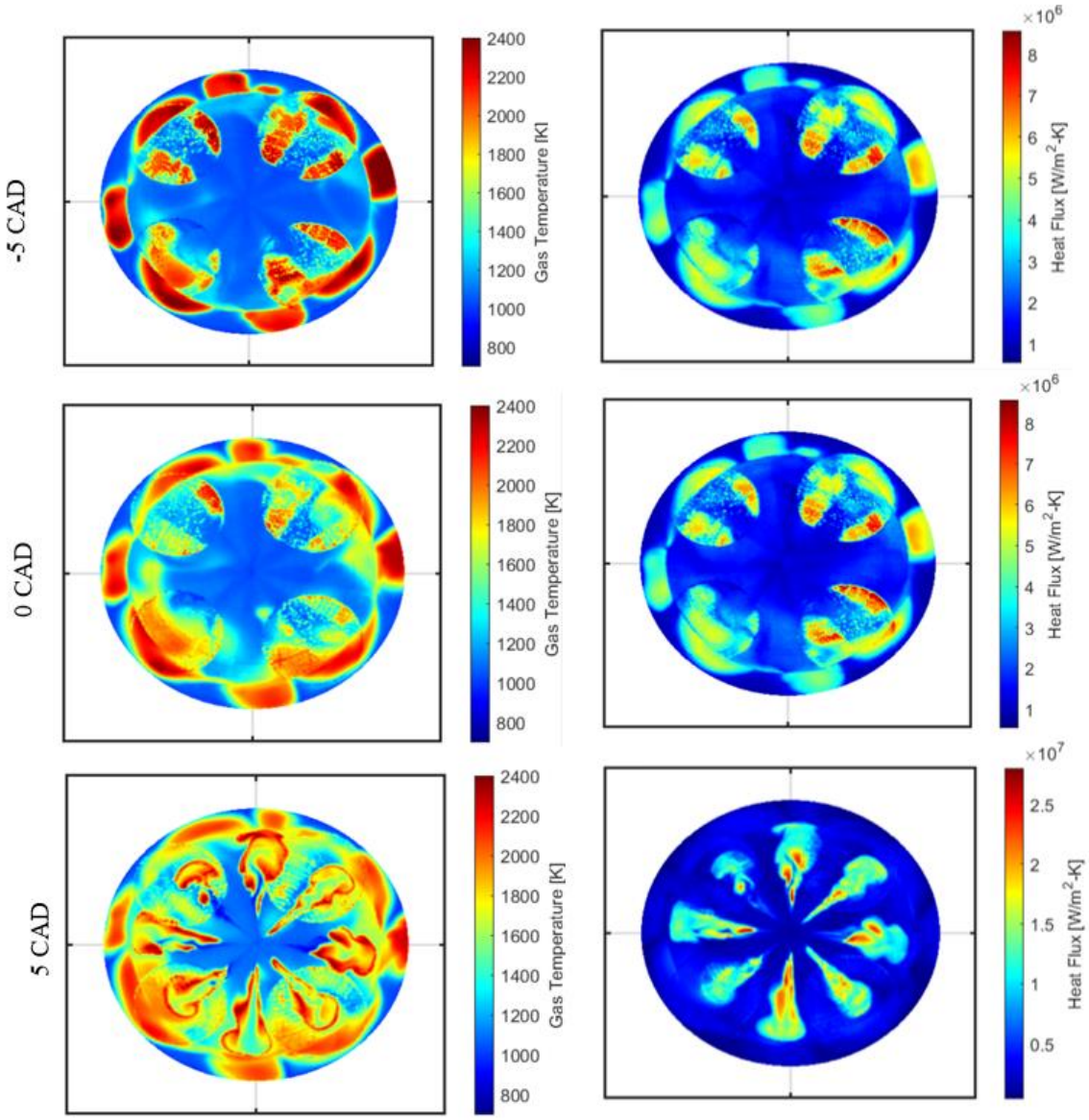

Figure 19: Near-wall gas temperature (left) and heat flux (right) at 0 CAD, 5 CAD and 10 CAD aTDC for 15 bar conditions

We can see that at -5 CAD, there are hot spots (red areas) where the temperature is the highest. As the piston moves from -5 CAD to 5 CAD, these hot areas spread around, showing how the heat is moving in the cylinder. The heat flux shows how much heat is moving from the engine's gases to the walls. A higher heat flux means more heat is being transferred. The color scale here also goes from blue to red, with red showing higher heat flux. At -5 CAD, the heat flux is

concentrated in specific areas, suggesting that these spots are where most of the heat transfer is happening. As the piston moves through TDC from -5 CAD to 5 CAD, the heat flux decreases, indicating less heat transfer to the walls.

These visualizations are particularly useful for engine designers and engineers, providing insight into how effective TBCs are in managing the engine's temperatures. The goal is for TBCs to reduce the amount of heat loss from the gases to the walls, improving engine efficiency. By understanding how the heat distribution and transfer change throughout the engine cycle, engineers can better design engines that perform optimally under various operating conditions, ultimately leading to better fuel efficiency and reduced emissions.

The results for the comparison of several performance parameters for 6-bar, 10-bar and 15-bar conditions are provided in Table 5, Table 6, and Table 7, respectively. The combustion was phased a bit earlier with the addition of TBC, during the co-simulation iteration. Therefore, a slight reduction in intake temperature was done to match the combustion phasing. At the 6-bar condition, both uncoated and coated pistons show higher net indicated mean effective pressure (IMEP) compared to experimental results, with the coated piston slightly outperforming the uncoated.

Table 5: Performance parameters comparisons for uncoated and coated piston with experimental results at a net IMEP of 6 bar

Parameters	**Uncoated Metal Piston**	**TBC-Coated Piston**	**Experiment**
Net IMEP [bar]	6.28	6.31	5.85±0.04
IVC Pressure [bar]	1.41	1.41	1.42±0.11

IVC Temperature [K]	421	420	426±10
Peak Pressure [bar]	76.35	76.3	76.41±0.10
MPRR [bar/CAD]	5.44	5.21	5.92±1.01
Net fuel efficiency [%]	42.12	42.28	44.35±0.11
Net thermal efficiency [%]	42.35	42.79	44.7±0.15
Gross fuel efficiency [%]	42.7	43	45.1±0.11
Combustion efficiency [%]	99.67	98.80	99.29±0.1
CA50 [CAD aTDC]	7.9	8	8.2±0.1
Exhaust Temperature [K]	658.27	661.51	648.54±10

The comparison of uncoated and TBC-coated pistons across different conditions—6 bar, 10 bar, and 15 bar—reveals the impact of coatings on engine performance metrics. These coatings aim to enhance thermal efficiency, reduce thermal stresses, and improve overall engine performance.

The intake valve closure (IVC) pressure and temperature remain largely unaffected by the coating, suggesting its minimal impact at this level. Peak pressures are closely matched across all variants, while the mean pressure rise rate (MPRR) is reduced in the TBC-coated piston, indicating a smoother combustion. Efficiency metrics—net fuel conversion, thermal, and gross fuel conversion efficiencies—are improved with the TBC, albeit still below the experimental values. The TBC leads to a slight delay in combustion, as evidenced by shifts in CA50 (crank angle at 50% fuel burn) and increased exhaust temperatures, likely due to reduced heat loss. For the 10-bar condition, the slight increases in net IMEP for TBC-coated pistons demonstrate the coating's effectiveness under higher loads.

Table 6: Performance parameters comparisons for uncoated and coated piston with experimental results at net IMEP 10 bar

Parameters	**Uncoated Metal Piston**	**TBC-Coated Piston**	**Experiment**
Net IMEP [bar]	10.74	10.78	9.84±0.04
IVC Pressure [bar]	1.82	1.81	1.83±0.11
IVC Temperature [K]	383	381	370±10
Peak Pressure [bar]	118.44	119.72	116.11±0.10
MPRR [bar/CAD]	10.86	9.8	10.34±1.01

Net fuel efficiency [%]	44.82	45.31	43.68±0.11
Net thermal efficiency [%]	45.05	45.5	44.31±0.15
Gross fuel efficiency [%]	45.33	45.82	45.65±0.11
Combustion efficiency [%]	99.48	99.69	98.66±0.1
CA50 [CAD aTDC]	7.3	7	7.5±0.1
Exhaust Temperature [K]	682.92	697.25	662.89±10

Peak pressures are higher in the coated pistons, which could be due to improved combustion chamber sealing or thermal management. The coated pistons also show lower MPRR, suggesting more controlled combustion. Efficiency metrics are notably better in the coated pistons, highlighting the benefits of TBC in enhancing engine performance. The coated pistons exhibit higher combustion efficiency and earlier CA50, aligning with the aim to match combustion phasing. Additionally, higher exhaust temperatures in coated pistons are consistent with reduced heat transfer to the piston. At the 15-bar condition, the improvements continue with marginally higher net IMEP in TBC-coated pistons, indicating slight power generation enhancements at this pressure.

Table 7: Performance parameters comparisons for uncoated and coated piston with experimental results at net IMEP 15 bar

Parameters	**Uncoated Metal Piston**	**TBC-Coated Piston**	**Experiment**
Net IMEP [bar]	15.30	15.51	14.73±0.04
IVC Pressure [bar]	2.39	2.39	2.37±0.11
IVC Temperature [K]	381	384	370±10
Peak Pressure [bar]	154.31	159.27	148.97±0.10
MPRR [bar/CAD]	13.47	21.52	11.80±1.01
Net fuel efficiency [%]	43.15	43.71	44.35±0.11
Net thermal efficiency [%]	43.37	43.84	44.70±0.15
Gross fuel efficiency [%]	43.4	43.96	45.65±0.11

Combustion efficiency [%]	99.47	99.72	99.52±0.1
CA50 [CAD aTDC]	6.8	7	7.9±0.1
Exhaust Temperature [K]	714.23	735.59	697.25±10

Similar IVC pressure and temperature across variants suggest the TBC coating's limited impact on intake conditions. The TBC-coated pistons show reduced MPRR, reflecting gentler pressure rises during combustion, and slight improvements in net and thermal efficiencies over uncoated pistons, although experimental values still outperform them. Combustion efficiency remains identical between uncoated and coated pistons, with both slightly lower than the experimental setup. The earlier CA50 in coated pistons suggests minor shifts in combustion timing, while higher exhaust temperatures and indicated specific fuel consumption (ISFC) in coated pistons could indicate its influence on fuel consumption and heat management strategies.

Overall, TBC-coated pistons generally exhibit improved efficiency and a more controlled combustion process across the tested conditions. These enhancements are accompanied by higher exhaust temperatures, underscoring the significant changes in heat transfer dynamics introduced by thermal barrier coatings.

The thermal efficiency for 10 bar and 15 bar conditions was predicted to be higher than the experiment for the TBC-coated piston but for 6 bar conditions, it was lower. On comparing the cumulative heat transfer through the piston, it was found that about 17% reduction of heat loss due

to the temperature swing phenomenon of TBCs for 10-bar conditions. As compared to conventional SI and diesel combustion studies, we have seen a reduction of roughly about 7% and 10%, respectively [33, 34]. However, the 17% reduction in heat transfer only translated to a 0.5 percentage point improvement in efficiency. Figure 19 shows cumulative heat transfer through uncoated and coated pistons for 6-bar conditions. It depicts how TBC affect the heat transfer characteristics of pistons in GCI combustion mode. For the 6-bar condition, the graph indicates that the heat transfer for the coated piston closely follows that of the uncoated one until the combustion phase.

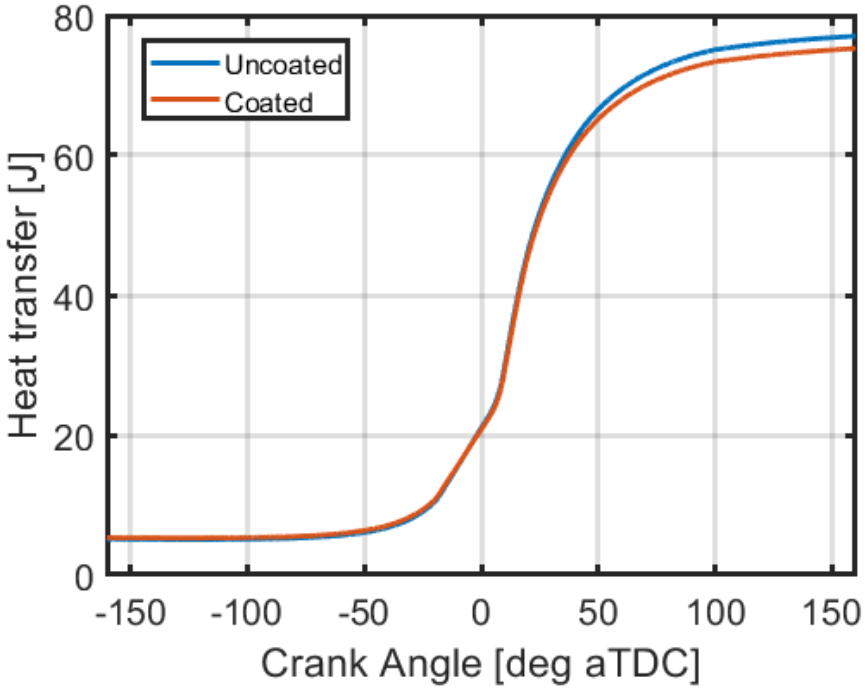

Figure 20: Cumulative heat transfer through piston for uncoated (blue) and coated (red) at 6-bar conditions

During combustion, the coated piston shows a reduced rate of heat transfer, which becomes more pronounced at the peak of combustion. This suggests that the TBC is effective at insulating the piston, reducing the heat flow from the combustion gases to the piston surface. After the peak,

the difference in heat transfer between the coated and uncoated piston narrows, indicating that the insulative effect of the coating is most significant during the high-temperature phase of the cycle. Figure 20 shows cumulative heat transfer through uncoated and coated pistons for 10-bar conditions. In the 10-bar condition, the cumulative heat transfer for both pistons begins to diverge earlier in the cycle compared to the 6-bar condition.

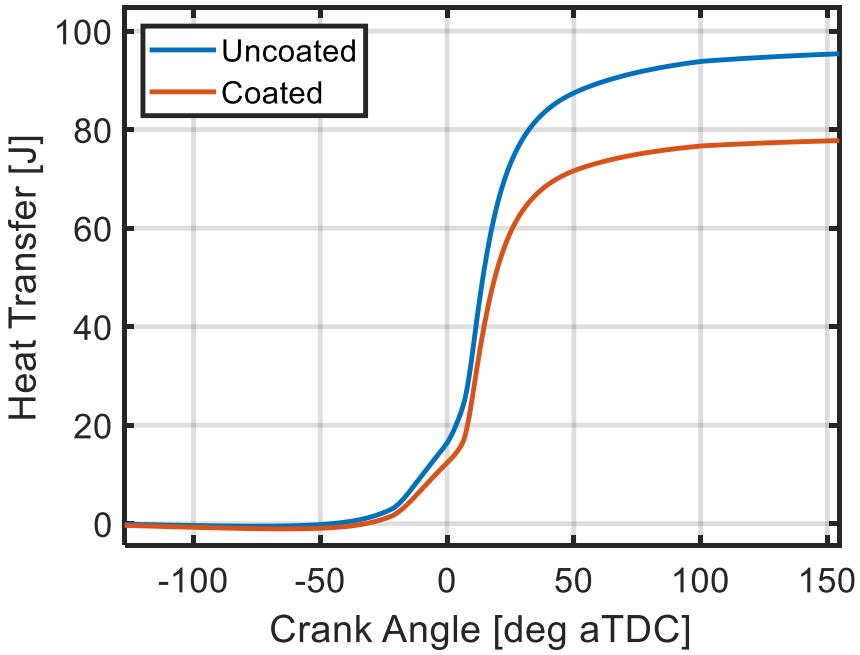

Figure 21: Cumulative heat transfer through piston for uncoated (blue) and coated (red) at 10-bar conditions

The TBC coating displays a notable reduction in heat transfer throughout the combustion process. The reduction in heat transfer is attributed to the decreased temperature gradient between the combustion gases and the piston surface due to the insulative properties of the coating. The difference in temperature between the gas and the piston wall is around 100K at peak combustion, showing the coating's effectiveness in maintaining a lower surface temperature on the piston,

which is likely contributing to the reduced heat transfer. Figure 21 shows cumulative heat transfer through uncoated and coated pistons for 15-bar conditions. At the 15-bar condition, the graph shows an even more substantial difference in heat transfer between the uncoated and coated pistons, starting before the combustion phase and continuing past the peak.

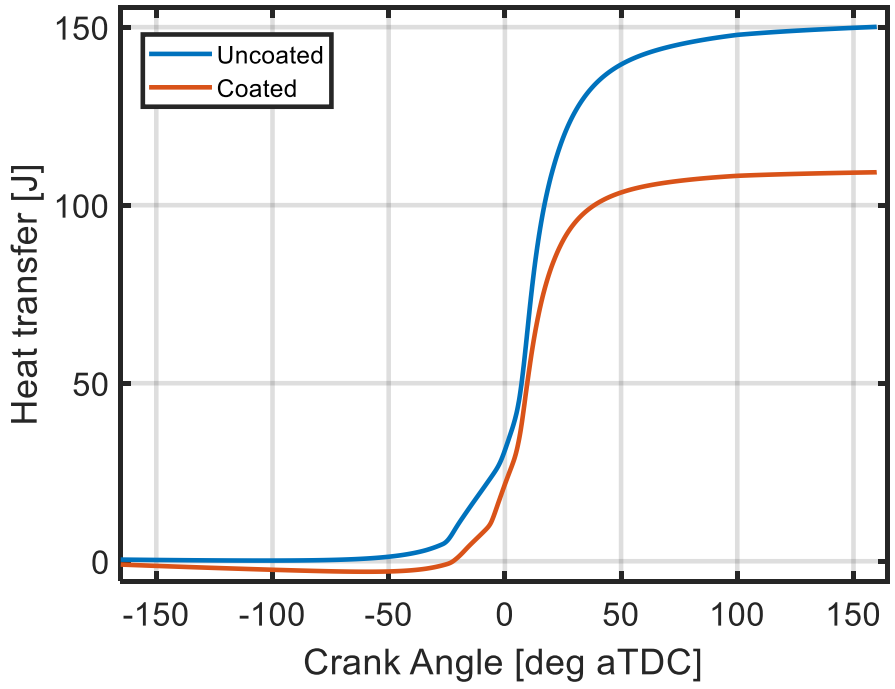

Figure 22: Cumulative heat transfer through piston for uncoated (blue) and coated (red) at 15-bar conditions

This indicates that as the pressure—and consequently the temperature—increases within the cylinder, the TBC becomes even more effective at reducing heat transfer. This is crucial at higher pressures, as the thermal loads are significantly greater, and the ability of the TBC to insulate the piston from these high temperatures can lead to improvements in the piston's lifespan and overall engine efficiency. This reduction in heat transfer is due to the reduction in the difference between the gas and wall temperatures during combustion.

Thus, the heat transfer through the piston demonstrates that the TBC effectively reduces the rate of heat transfer during the combustion phase across all pressures, with its benefits becoming more pronounced as the operating pressure—and therefore the temperature and thermal loads—increases. The TBC's impact is reflected in its ability to lower the piston surface temperature relative to the gas temperature, resulting in a smaller temperature gradient and, thus, reduced heat flow. Since a greater heat loss reduction at 15 bar conditions still accounted for only 0.5 percentage points improvement in efficiency, some heat might have gone to the exhaust side increasing the exhaust temperature which can be observed for all three operating conditions. This reduction in heat transfer to the piston can lead to improved engine performance, as it can reduce thermal stresses and increase the efficiency of the combustion process.

Figure 22 illustrate the difference in temperature between the gas and the piston surface over the engine cycle, comparing uncoated and TBC-coated pistons at 6 bar conditions. This temperature difference is crucial for understanding the heat transfer dynamics and the efficiency of the coating. At the 6-bar condition, the temperature difference curves for both uncoated and coated pistons follow a similar trend, with the uncoated piston maintaining a slightly higher temperature difference throughout the cycle.

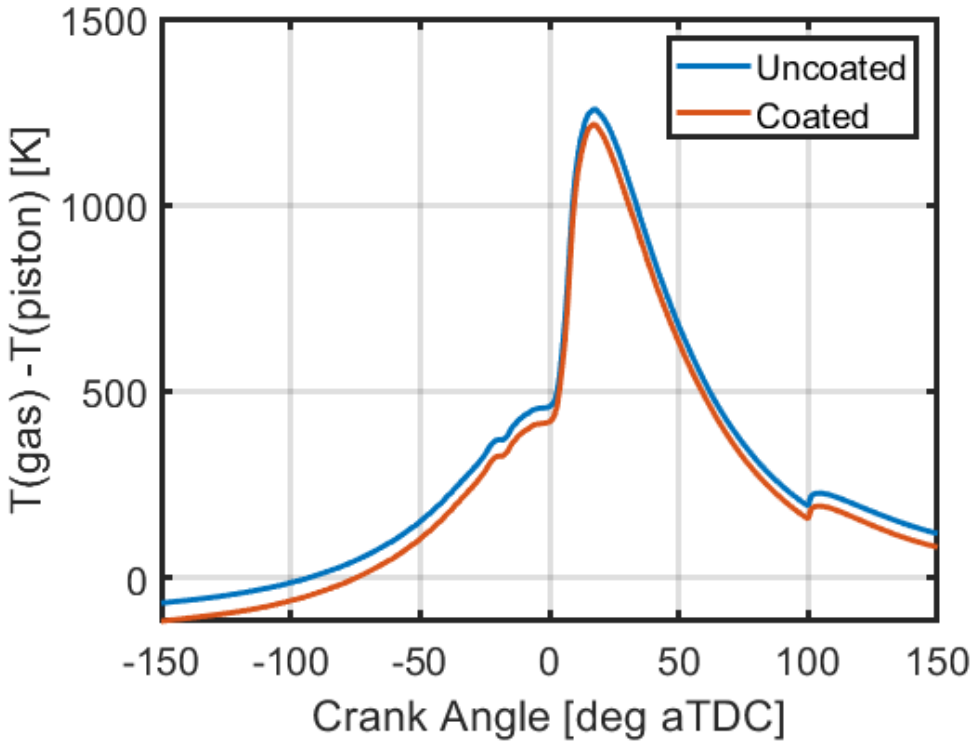

Figure 23: Gas temperature minus piston temperature for uncoated (blue) and coated (red) at 6-bar conditions

This suggests that the surface of the coated piston is hotter compared to the uncoated one during the combustion phase. Since heat transfer depends on the temperature difference between the gas and the piston, a higher piston surface temperature in the coated piston could lead to reduced heat transfer to the piston during this phase. It appears that the TBC's insulating effect becomes less pronounced at lower pressure conditions, as evidenced by the smaller temperature difference.

Figure 24 and Figure 25 shows the near wall gas temperature minus piston surface temperature for uncoated and coated pistons for 6 bar conditions during peak combustion at 15 CAD aTDC. Since the near-wall gas temperature is higher than the piston surface temperature, it suggests effective heat transfer from the combustion gases to the piston, minimizing heat losses.

Comparing the uncoated and coated pistons, the average temperature difference was observed higher for uncoated pistons. The higher temperature difference was observed to the region on the surface where the spray targets which is around the bowl and then gradually shifting towards the squish region as we move forward in the engine cycle. In the center region, a lower temperature difference was observed. On taking the average of this difference for all the nodes on the piston surface, the peak combustion temperature was found to be about 45K higher for the uncoated piston. This suggests that the heat transfer losses from the piston were reduced to 5% for the coated piston.

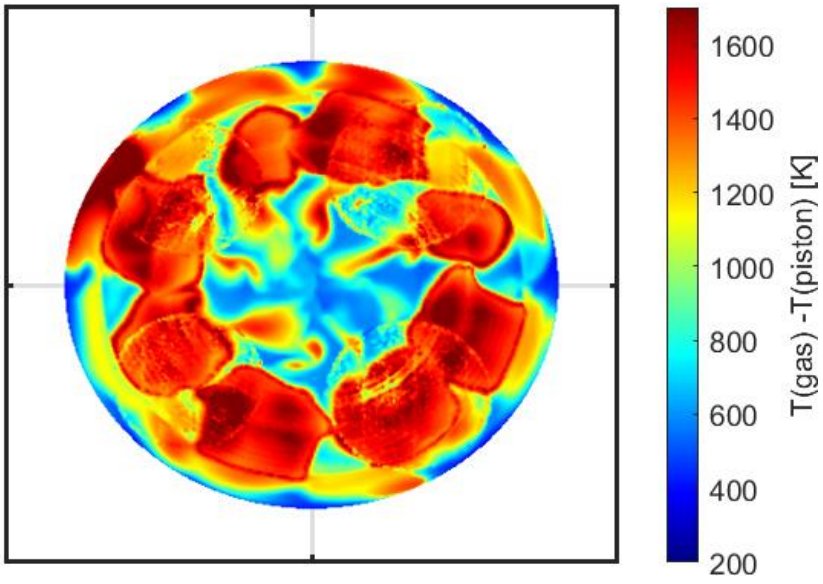

Figure 24: Gas temperature minus piston temperature for uncoated piston on the piston surface at 15 CAD aTDC for 6 bar conditions

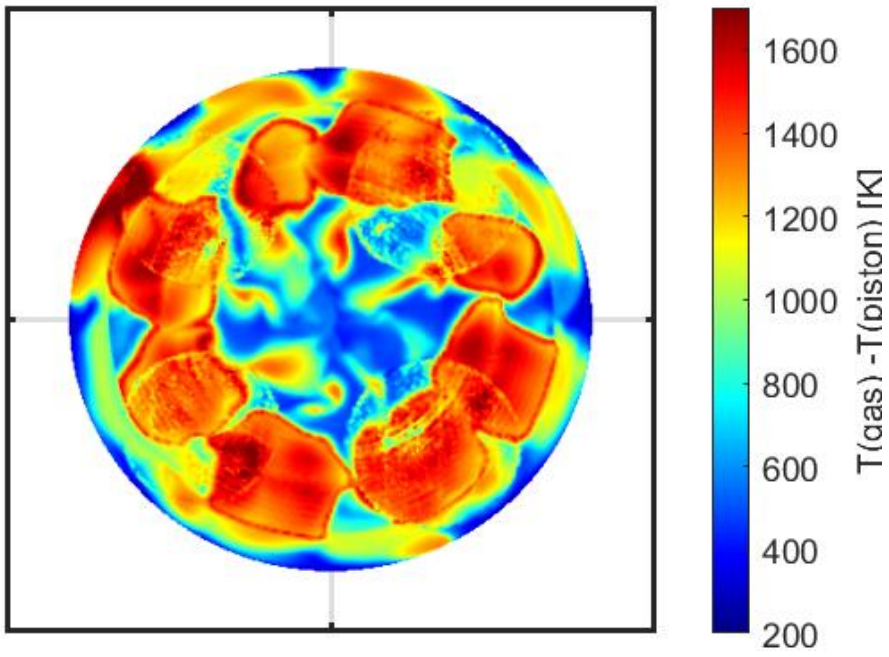

Figure 25: Gas temperature minus piston temperature for coated piston on the piston surface at 15 CAD aTDC for 6 bar conditions

Figure 23 illustrates the difference in temperature between the gas and the piston surface over the course of the engine cycle, comparing uncoated and TBC-coated pistons at 10 bar conditions.

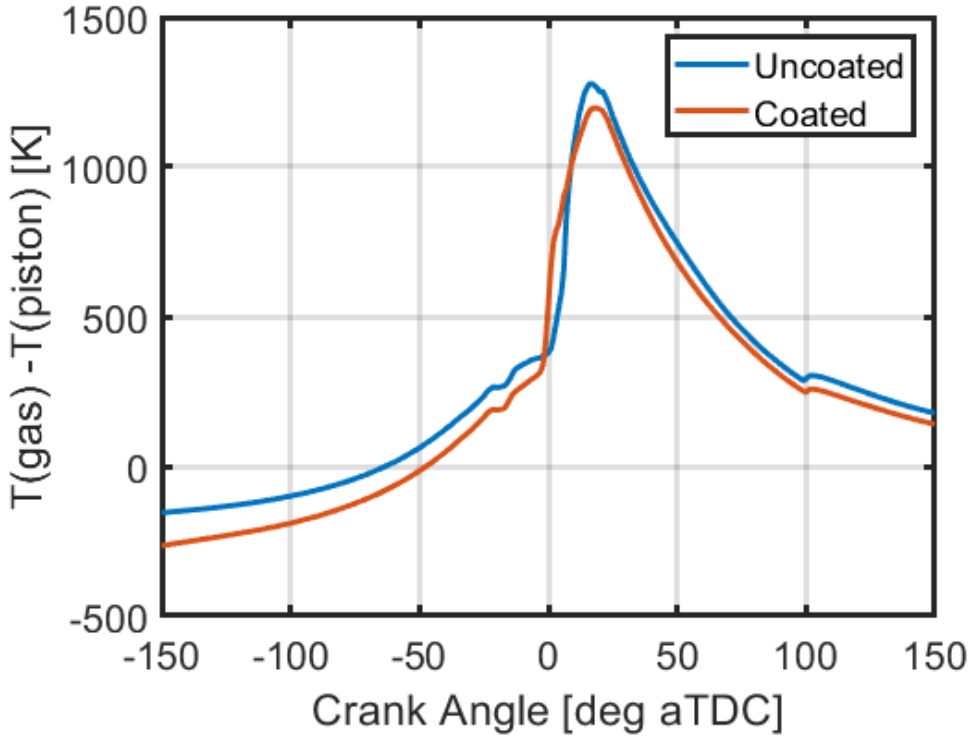

Figure 26: Gas temperature minus piston temperature for uncoated (blue) and coated (red) at 10-bar conditions

For the 10-bar condition, the trend continues, but the difference in temperature between the gas and the piston surface increases as the load increases. The peak difference for the coated piston indicates that the surface temperature is considerably higher than that of the uncoated piston during combustion. This can be interpreted as the TBC effectively raising the surface temperature, which could potentially lead to a heat transfer reduction to the piston during combustion.

Figure 27 and Figure 28 show the near wall gas temperature minus piston surface temperature for uncoated and coated pistons for 10 bar conditions during peak combustion at 15 CAD aTDC. The temperature difference is higher to the periphery of the piston surface where the spray targets. The spatial temperature difference ranges from 200K to 1600K which reflects the thermal conditions on the piston surface. The region in the center is comparatively cooler and has the temperature difference average in the range of about 800K for the uncoated case and about

750K for the coated case. As compared to the 6 bar conditions, the temperature difference for coated and uncoated cases was higher and was near about 100K during peak combustion. This suggests that the heat transfer losses from the piston were reduced to about 17% for the coated piston as explained above.

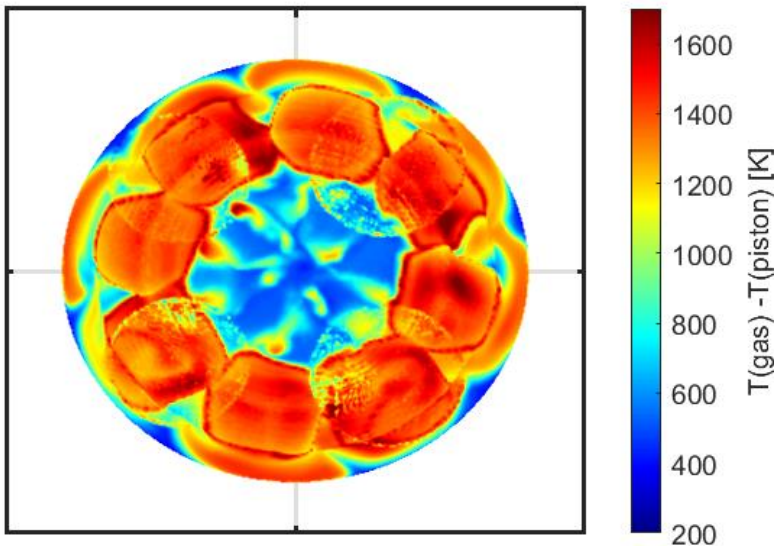

Figure 27: Gas temperature minus piston temperature for uncoated piston on the piston surface at 15 CAD aTDC for 10 bar conditions

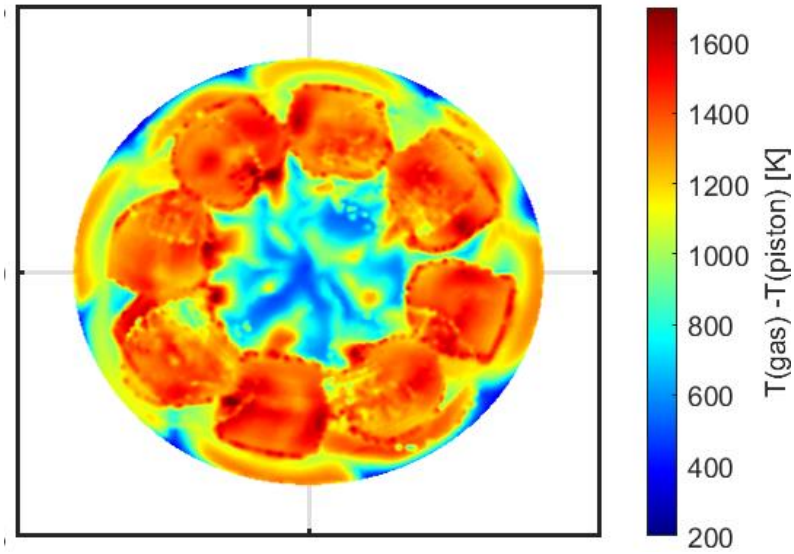

Figure 28: Gas temperature minus piston temperature for coated piston on the piston surface at 15 CAD aTDC for 10 bar conditions

Figure 24 illustrates the difference in temperature between the gas and the piston surface throughout the engine cycle, comparing uncoated and TBC-coated pistons at 15 bar conditions. At the 15-bar condition, the difference in temperature between the gas and the piston surface for the coated piston further increases, suggesting even greater heat transfer reduction during combustion.

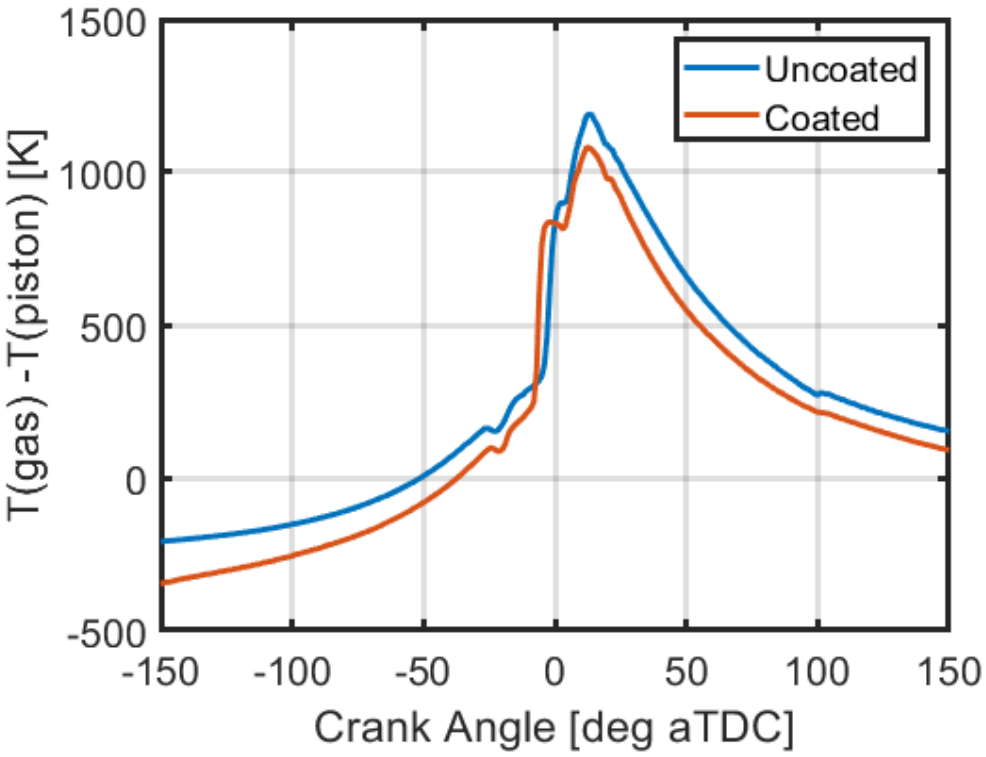

Figure 29: Gas temperature minus piston temperature for uncoated (blue) and coated (red) at 15-bar conditions

Figure 30 and Figure 31 show the gas temperature the near wall gas temperature minus piston surface temperature for uncoated and coated pistons for 15 bar conditions during peak combustion at 15 CAD aTDC. Cooler regions in the center suggest areas where the fuel-air mixture is less concentrated or where there is an increase in heat transfer losses. The temperature difference distributions were almost similar to the 6-bar and 10-bar conditions. It was observed greater at the region around the periphery of the piston

surface suggesting a greater reduction in the heat transfer. On comparing 15 bar uncoated and coated cases, the average temperature difference was more than 100K for the coated piston as compared to the uncoated piston. Similarly, as compared to 6-bar and 10-bar conditions, the temperature difference was significantly higher suggesting a higher reduction in heat transfer losses.

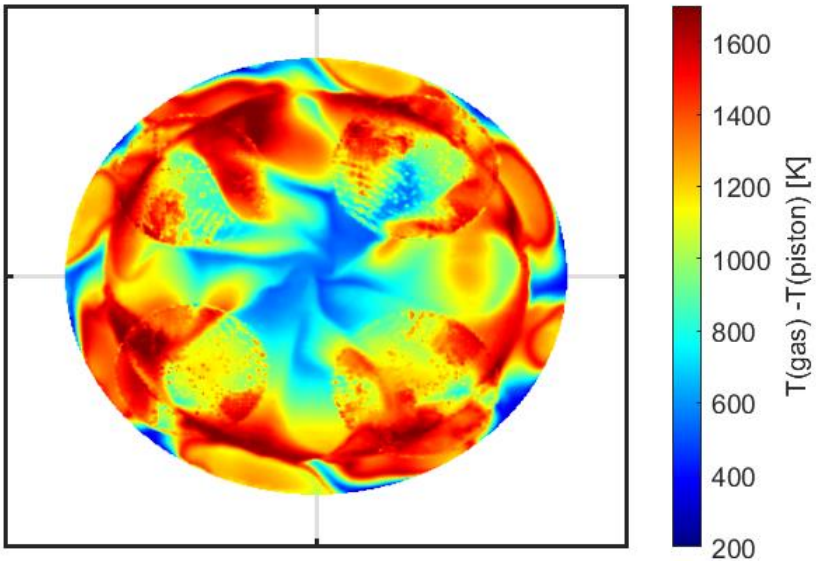

Figure 30: Gas temperature minus piston temperature for uncoated piston on the piston surface at 15CAD aTDC for 15 bar conditions

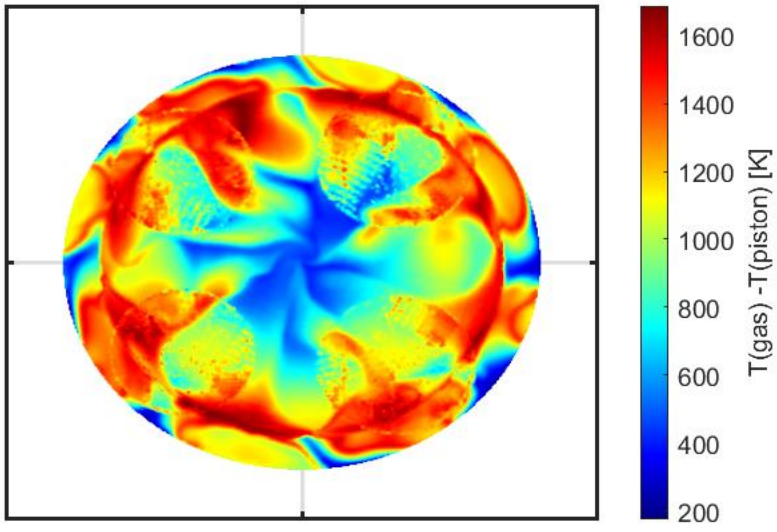

Figure 31: Gas temperature minus piston temperature for coated piston on the piston surface at 15CAD aTDC for 15 bar conditions

As the pressure and temperature within the cylinder rise, the TBC's role in insulating the piston seems to result in a significantly hotter piston surface compared to the uncoated piston. This effect may have implications for thermal management and engine efficiency, particularly at high loads where excessive heat can affect performance and engine longevity.

The observed trend suggests that while TBC reduces the temperature gradient and heat transfer during most parts of the engine cycle, during the combustion phase, the surface temperature of the coated piston exceeds that of the uncoated piston, leading to potentially lower heat transfer rates. This could have a complex impact on engine performance, where the insulating benefits of TBC might be countered by increased heat transfer during combustion.

When we compared how heat moves near the walls of the engine between a regular metal piston and one with TBC, we found that the heat transfer was mostly the same during most of the engine's cycle. However, during combustion, the coated piston had lower heat transfer. This means that the surface of the coated piston gets hotter during combustion. This hotter surface affects how heat conduction pathways around the piston three dimensionally, especially during combustion. Researchers have shown that when the surface temperature of the coated piston reaches over 1000K, it changes the thermal behavior around the piston [33]. This change does not necessarily make the engine more efficient, especially at high load conditions. Some studies even showed that the engine might not run as efficiently at high load conditions when this happens [48, 49]. However, in our study, we used CFD and FEA to look at thermal behavior around the piston, and we found that using a grid size of 1mm around the piston showed better efficiency, suggesting that our previous grid size might not have been detailed enough. In the future, we plan to use more advanced CFD models to look even closer at how heat moves around the piston, especially at higher operating loads.

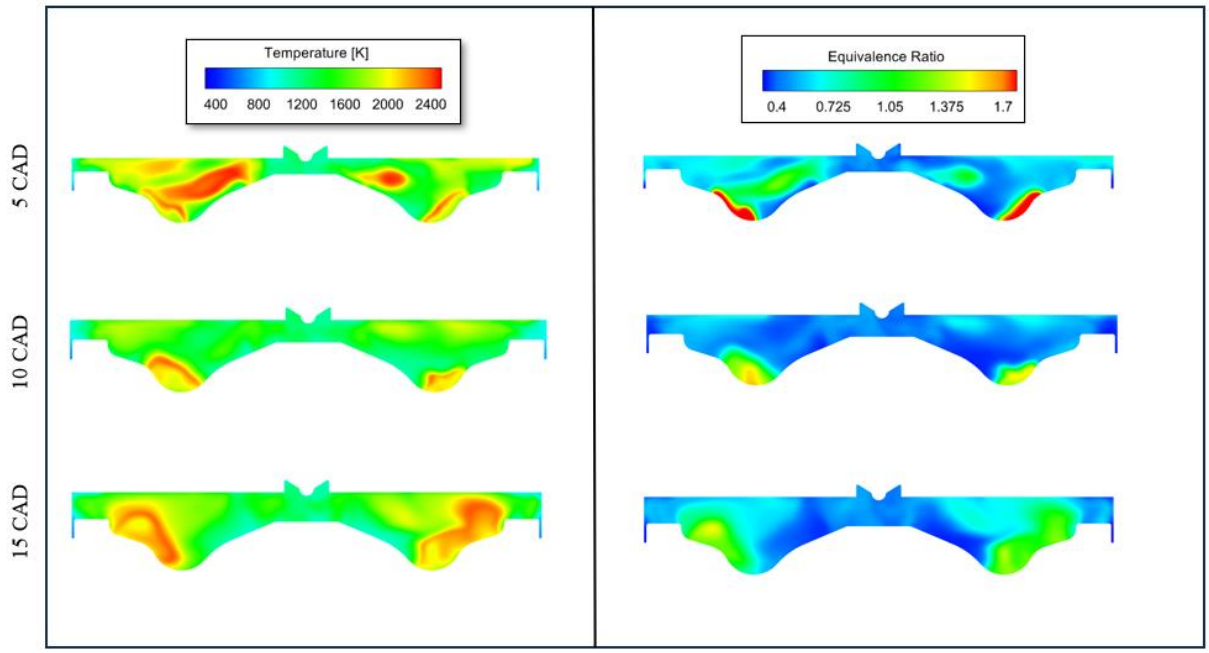

Figure 32: Cut-plane visualizations for temperature (left) and equivalence ratio (right) distributions at 5, 10, and 15 CAD aTDC for coated piston at 6-bar conditions

The cut plane visualizations for a coated piston at 6, 10 and 15 bar conditions offer a detailed look into the in-cylinder processes of a GCI engine. Figure 32 shows temperatue and equivalence ratio distributions for (Y-Y cut plane) for coated piston at 6 bar. In GCI combustion, the air is compressed and fuel is injected in toward the end of compression stroke. The distribution of fuel and air within the cylinder, characterized by the equivalence ratio, and the temperature distributions are key factors that influence combustion quality, emissions, and engine efficiency. Fuel injection strategy is critical in GCI because it affects the formation of combustible mixtures and temperature stratification within the cylinder. Spray patterns directly influence the equivalence ratio distributions. Ideally, fuel should be distributed evenly to create a homogenous mixture, but practical limitations often result in regions of rich and lean mixtures.

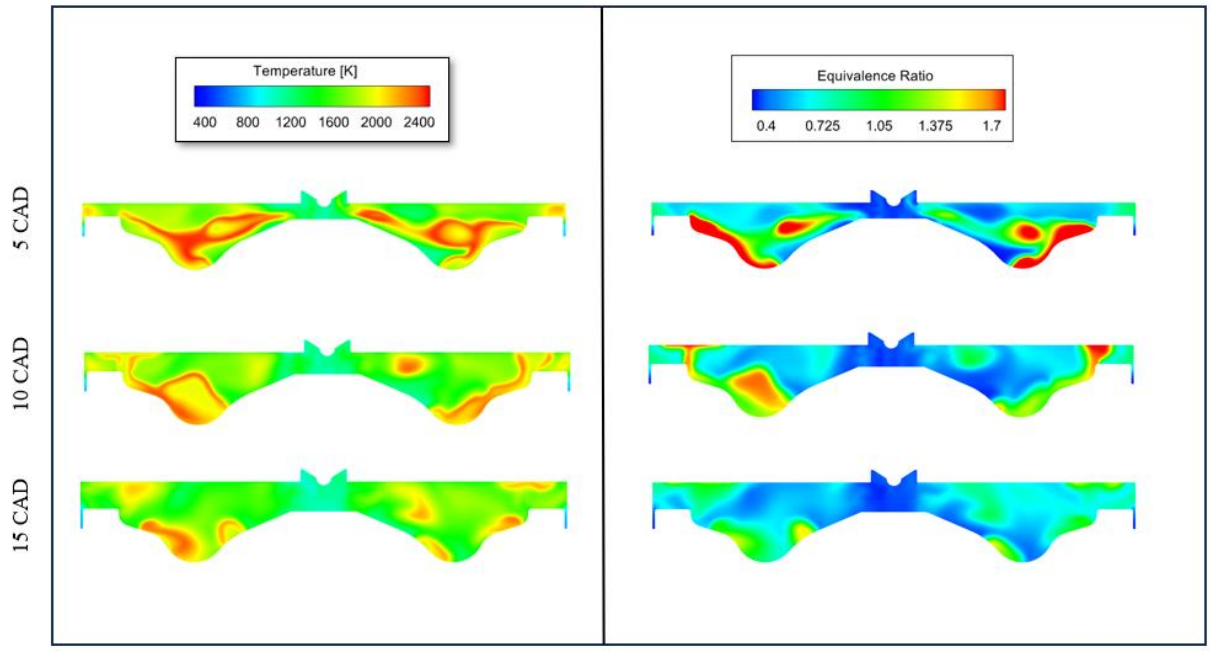

Figure 33: Cut-plane visualizations for temperature (left) and equivalence ratio (right) distributions at 5, 10, and 15 CAD aTDC for coated piston at 10-bar conditions

Figure 33 shows temperature and equivalence ratio distributions for (Y-Y cut plane) for coated piston at 10 bar. Rich regions contain more fuel than necessary for complete combustion with the available air, leading to incomplete combustion and higher emissions of unburned hydrocarbons and particulate matter. Lean regions, on the other hand, have excess air, which can result in higher nitrogen oxide emissions due to higher combustion temperatures but can also improve fuel efficiency. Figure 34 shows temperature and equivalence ratio distributions for (Y-Y cut plane) for coated piston at 15 bar. From the visualizations, it appears there are both rich and lean zones present within the combustion chamber. Such heterogeneity can arise from various factors, such as fuel spray dynamics, interaction with the piston bowl, and local air movement.

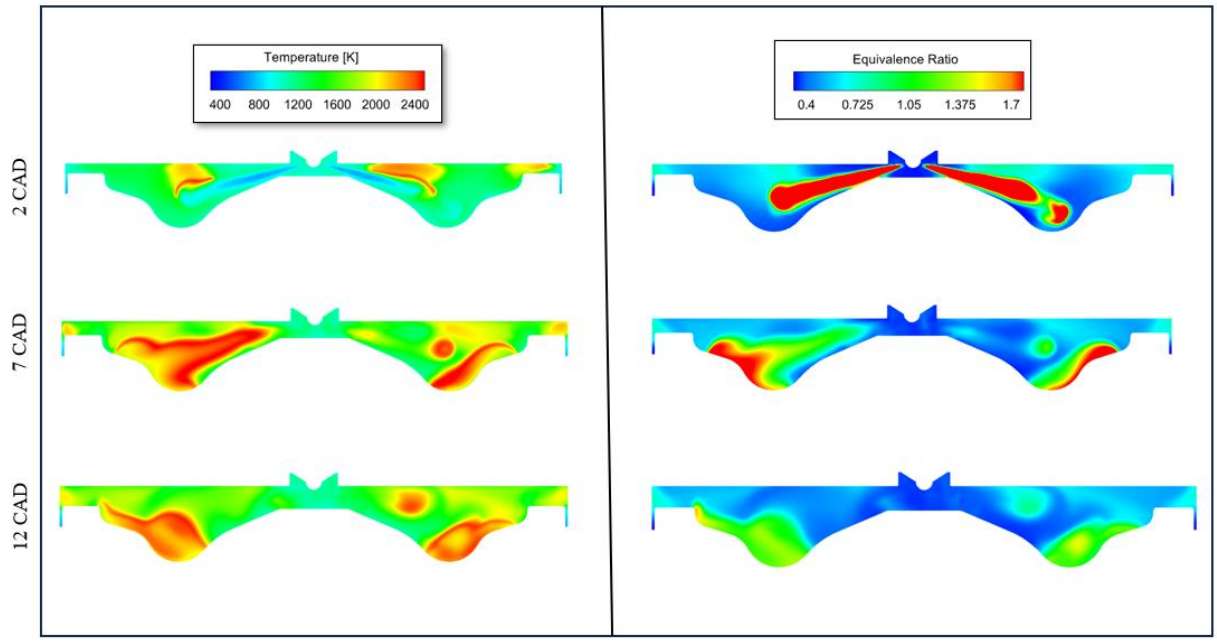

Figure 34: Cut-plane visualizations for temperature (left) and equivalence ratio (right) distributions at 2, 7, and 12 CAD aTDC for coated piston at 15-bar conditions

The temperature distributions are key to understanding the efficiency and effectiveness of the TBC. In areas where the temperature appears red or high on the scale, the TBC must withstand high thermal loads. It must provide insulation to prevent excessive heat loss through the piston walls, thereby ensuring that combustion temperatures remain high enough to ensure efficient combustion. The blue and green areas indicate cooler regions, which are less of a thermal management concern but still critical for overall combustion. If these areas are too cool, the fuel may not ignite properly, leading to incomplete combustion and poor efficiency. By insulating the combustion chamber, TBCs help maintain high combustion temperatures, which is essential for the GCI combustion, as it relies on heat to ignite the fuel-air mixture. TBCs can also protect the piston from the hot spots that can occur in rich mixture zones, potentially preventing local overheating and material degradation. However, the effectiveness of TBCs can be influenced by the distribution of rich and lean areas. In rich regions, where temperatures are higher due to excess

fuel burning, TBCs must be particularly effective at insulating the piston to prevent thermal runaways and knock. In lean regions, TBCs can help sustain combustion by keeping heat within the cylinder, which might otherwise be too cool for efficient combustion.

In the visualizations, especially at the higher 10 bar condition, there are noticeable hot zones where the TBC will be most stressed. The performance of the TBCs in these areas is crucial for engine longevity and efficiency. If the TBCs deteriorate, the thermal management capabilities of the engine could be compromised, leading to reduced efficiency and potential engine damage due to overheating.

CHAPTER FOUR

CONCLUSIONS AND RECOMMENDATIONS FOR FUTURE WORK

The study is on the co-simulation of CFD and FEA, which has led to a distinct understanding of TBCs' impact on GCI combustion mode. The computer models CFD and FEA were used to study how a coating gadolinium zirconate TBC affects heat transfer and efficiency in GCI combustion. These models were linked together so they could work together to understand what happens inside the engine piston. It took three iterations to get the models to agree on how the piston behaves. In the end, the surface of the TBC-coated piston got hotter than a regular metal piston, reaching 930K with a swing of 100K, compared to 619K for the metal piston for medium load operating conditions. We also adjusted the timing of combustion to match the real-world conditions better. The TBC reduced heat loss by 5% for 6 bar conditions, and about 17% for 10-bar conditions, and according to our models, it should improve efficiency by 0.5 percentage points. Similarly, for the 15-bar coated case, the heat transfer loss was found to reduce about 36%. However, when these coating were experimentally tested in real engines, there was a slight efficiency improvement at low loads, but a slight efficiency penalty at the higher load operating conditions of 15 bar [51]. It is found that this trend is due to increase in near wall heat transfer coefficient caused by “convection vive” [52] affecting the near-wall thermal boundary layer. At a load of 10 bar, the efficiency was the same with or without the coating.

- The application of Gadolinium Zirconate (GdZr) as a TBC is shown to significantly influence the temperature regulation within the combustion chamber. It manages to contain the surface temperature fluctuations, which in turn impacts the thermal efficiency positively by mitigating heat loss through the piston walls.

- The simulations predicted a modest but notable improvement in thermal efficiency attributable to the TBC application. However, this theoretical efficiency gain was not seen in experimental outcomes, indicating that real-world complexities might not be fully captured by the simulation models.
- The inconsistency between the predicted and actual efficiency improvements highlights the complex nature of heat transfer in GCI and suggests a potential gap in the simulation's ability to capture all relevant heat transfer mechanisms.
- There is a clear indication from the simulation results that TBCs have the potential to reduce heat transfer through the piston by a considerable margin, demonstrating the role TBCs could play in thermal management and performance optimization in GCI.

There are several paths for further research that could expand the current understanding of TBCs.

- To improve the match between simulated and actual engine behavior, a more extensive validation of the CFD and FEA models is recommended. This could involve comparing simulation results with experimental data across a wider range of operating scenarios, engine speeds, and loads.
- The study suggests the necessity for more sophisticated simulation methodologies that can more accurately model the distinct heat transfer phenomena, especially the convective heat transfer that seems to play a critical role in engine wall temperature dynamics.
- A closer look into the turbulence models and fuel injection simulations could help in enhancing the predictive accuracy of the models. Since these factors have a significant influence on the combustion process, refining these models could lead to better optimization of engine performance.

- There is room for investigation into different TBC materials and configurations. These studies could provide insights into the thermal and mechanical properties that best suit the high-load and high-temperature conditions of GCI.
- Given the high temperatures and pressures involved in GCI, a comprehensive analysis of the thermo-mechanical stresses experienced by TBCs could provide valuable information on their durability and operational longevity.
- Applying the findings to real-world GCI and assessing the impact on actual vehicle performance would be the ultimate test of the TBCs' viability. These studies should focus on long-term efficiency, emissions profiles, and durability under typical driving conditions.
- Conducting more experimental tests that examine a variety of TBC thicknesses and compositions can help identify the most effective TBC application for GCI, balancing performance benefits with practical challenges. The "penetrative depth" tells us how deep the heat changes go into a coating during an engine's operation. Basically, if the coating is thicker than this depth, making it thicker does not change how much the surface temperature swings up and down, except it might go down a bit because less heat is transferred. However, if the coating is thinner than this depth, making the coating thicker will make the surface temperature change more [53].

By following these recommendations, future work can not only validate the findings of this thesis but also propel the application of TBCs from theoretical modeling to practical engine improvements. The goal would be to deploy TBCs in GCI engines widely, enhancing fuel efficiency, and reducing emissions, thus contributing to the development of more sustainable automotive technologies.

REFERENCES

[1] Uchida, N., “A review of thermal barrier coatings for improvement in thermal efficiency of both gasoline and diesel reciprocating engines”, *International Journal of Engine Research,* vol. 23 (1) pp. 3-19, 2022.

[2] Zheng, Z., Chen, P., Zhang, F., Yao, M., Wang, H., Liu, H., “Experimental Study on the effect of thermal barrier coated (TBC) piston on combustion of gasoline compression ignition (GCI)”, *Applied Thermal Engineering,* 24 July, 2022. https://doi.org/10.1016/j.applthermaleng.2022.119068

[3] Yan, Z., Levi, A., Zhang, Y., Sellnau, M., Filipi, Z., Lawler, B., “A numerical evaluation and guideline for thermal barrier coatings on gasoline compression ignition engines”, *International Journal of Engine Research,* vol. 21 (5), pp. 2206-2222, 2023.

[4] Powell, T., O’ Donnell, R., Hoffmann, M., Filipi, Z., “Impact of a Yttria-Stabilized Zirconia Thermal Barrier Coating on HCCI Engine Combustion, Emissions, Efficiency”, *Journal of Engineering for Gas Turbines and Power,* vol.139, November 2017.

[5] Vedpathak, K., “Experimental Study on the Impact of Low Thermal Inertia Thermal Barrier Coatings on PPCI-Diffusion GCI Combustion” (2023). *Clemson University*, *All Theses*, 4187

[6] Somhorst, J., Oevermann, M., “Effect of thermal barrier coating porosity on combustion and heat losses in a light duty diesel engine”, *International Journal of Engine Research,* 20 October 2023.

[7] Chauhan, N., Chauhan, K., “Thermal Barrier Coating system for Internal Combustion Engine application – A review”, *IOP Conference Series: Materials Science and Engineering*, 872, 012086.

[8] Yan, Z., Gainey, B., Gohn, J., Hariharan, D., Saputo, J., Schmidt, C., Callari, F., Sampath, S., Lawler, B., " The Effects of Thick Thermal Barrier Coatings on Low-Temperature Combustion", *SAE International Journal of Advances and Current Practices in Mobility* 2(4):1786-1799, 2020. https://doi.org/10.4271/2020-01-0275.

[9] Powell, T., Killingsworth, N., Hoffman, M., O'Donnell, R., Prucka, R., Filispi, Z., "Predicting the gas-wall boundary conditions in a thermal barrier coated low-temperature combustion engine using sub-coating temperature measurements," *International Journal of Powertrains*, 6(2):125-150, 2017, https://doi.org/10.1504/IJPT.2017.085679

[10] Cung, K., Moiz, A., Smith, E., Bitsis, D., Michlberger, A., Briggs, T., Miwa, J., "Gasoline compression ignition (GCI) combustion of pump-grade gasoline fuel under high compression ratio diesel engine", *Transportation Engineering,* 14 March, 2021. https://doi.org/10.1016/j.treng.2021.100066

[11] Agarwal, A., Solanki, V., Krishnamoorthi, M., "Gasoline compression ignition (GCI) combustion in a light-duty engine using double injection strategy", *Applied Thermal Engineering,* 5 January, 2023. https://doi.org/10.1016/j.applthermaleng.2023.120006

[12] Cung, K., Bitsis, D., Miwa, J., Smith, E., Briggs, T., Morris, A., Michlberger, A., Moiz, A., "Investigation of Gasoline Compression Ignition (GCI) Combustion in a High Compression-Ratio Heavy-duty Single-Cylinder Diesel Engine", *SAE Technical Paper,* 2021-01-0495, 2021, doi:10.4271/2021-01-0495.

[13] Liu, L., Zhang, Z., Liang, Y., Zhang, F., Yang, B., "Combustion stability control of gasoline compression ignition (GCI) under low-load conditions: A Review", *Applied Mathematics and Nonlinear Sciences*, vol. 6, 2021. https://doi.org/10.2478/amns.2021.1.00039

[14] Gainey, B., Gandolfo, J., Yan,Z., Vedpathak, K., Kumar, R., Jordan, E., Sellnau, M., Filipi, M., Lawler, B., “A two-material thermal barrier coating spatially tailored for high-efficiency GCI combustion”, *International Journal of Engine Research,* vol. 25 (1), pp. 156-169, 2024.

[15] Mao, B., Cheng, P., Liu, H., Zheng, Z., Yao, M., Gasoline compression ignition operation on a multi-cylinder heavy duty diesel engine," Fuel, vol. 215, pp. 339-351, 2018. https://doi.org/10.1016/j.fuel.2017.09.020

[16] Jiang, C., Huang, G., Liu, G., Qian, Y., Lu, X., “Optimizing gasoline compression ignition engine performance and emissions: Combined effects of exhaust gas recirculation and fuel octane number”, *Applied Thermal Engineering*, vol. 153, pp. 669-677, 2019. https://doi.org/10.1016/j.applthermaleng.2019.03.054

[17] Putrasari, Y., Lim, O., “A Review of Gasoline Compression Ignition: A Promising Technology Potentially Fueled with Mixtures of Gasoline and Biodiesel to Meet Future Engine Efficiency and Emission Targets”, *Energies*, MDPI, vol. 12(2), pp. 1-27, January, 2019.

[18] Hu, Y., Huang, Z., Wang, L., Sun, X., Chen, W., “Experimental study on combustion and emissions of a compression ignition engine fueled with gasoline”, *Advances in Mechanical Engineering*, vol.14(7), pp. 1-8.

[19] B. Dempsey, A., J. Curran, S., M. Wagner, R., “A perspective on the range of gasoline compression ignition combustion strategies for high engine efficiency and low NOx & soot emissions: effects of in-cylinder fuel stratification”, Oak Ridge National Laboratory, Oak Ridge, TN, USA.

[20] Cracknell, R., A. Cortijo, J., Dubois, T., Engelen, B., Maneulli, P., Pellegrini, L., Willaims, J., “Exploring a Gasoline Compression Ignition (GCI) engine concept”, RWTh Aachen University, December, 2014.

[21] Kalghatgi, G., Johansson, B., “Gasoline compression ignition approach to efficient, clean and affordable future engines”, *International Journal of Automobile Engineering,* vol. 232 (1), pp. 118-138.

[22] Dec, John E. "Advanced compression-ignition engines—understanding the in-cylinder processes." *Proceedings of the combustion Institute* 32, no. 2 (2009): 2727-2742.

[23] Yoshizawa, K.,Teraji, A., Aochi, E., Kubo, M., Kimura, S., “Numerical Analysis of Combustion in Gasoline Compression Ignition Engines”, *SAE International*, vol. 111(3), pp. 2664-2678.

[24] Hiraya, K., Kazuya, H., Urushihara, T., Iiyama, A., Itoh, T., “A Study on Gasoline Fueled Compression Ignition Engine ~ A Trail of Operation Region Expansion”, *Journal of Engines* (2002), pp. 854-862.

[25] Caputo, S., Millo, F., Boccardo, G., Piano, A., Cifali, G., Pesce, F., “Numerical and experimental investigation of a piston thermal barrier coating for an automotive diesel engine application”, *Applied Thermal Engineering,* 2019.

[26] Dimitrakopoulos, N., Belgiorno, G., Tuner, M., Tunestal, P., Di Blasio, G., “Effect of EGR routing on efficiency and emissions of a PPC engine”, Applied Thermal Engineering, vol. 152, pp. 742-750, 2019. https://doi.org/10.1016/j.applthermaleng.2019.02.108

[27] Kundu, P., Scarcelli, R., Som, S., Ickes A., Wang, Y., Kiedaisch, Rajkumar, M., "Modeling Heat Loss through Pistons and Effect of Thermal Boundary Coatings in Diesel Engine Simulations using a Conjugate Heat Transfer Model", *SAE Technical Paper* 2016-01-2235, 2016.

[28] Yan, Z., Gainey, B., Lawler, B., "A parametric modeling study of thermal barrier coatings in low-temperature combustion engines", *Applied Thermal Engineering,* 16 October, 2021.

[29] Taibani, A., Visaria, M., Phalke, V., Alankar, A., Krishnan, S., Analysis of Temperature Swing Thermal Insulation for Performance Improvement of Diesel Engines", *SAE International Journal of Engines* 12(2): pp. 117-127, 2019.

[30] Killingsworth, N., O'Donnell. R., Powell, T., Filipi, Z., Hoffmann, M., "Modeling the Effect of Thermal Barrier Coatings on HCCI Engine Combustion Using CFD Simulations with Conjugate Heat Transfer", *SAE Technical Paper,* 2019-01-0956, 2019.

[31] Babu, A., Koutsakis, G., Kokjohn, S., Andrie, M., "Experimental and Analyical Study of Temperature Swing Piston Coatings in a Medium-Duty Diesel Engine", *SAE International Journal of Advances and Current Practices in Mobility*, vol. 5, no. 1, pp. 235-248, 2022. https://doi.org/10.4271/2022-01-0442

[32] Josell, D., Bonevich, J., Nguyen, T., N. Johnson, "Heat transfer through nanoscale multilayered thermal barrier coatings at elevated temperatures", *Surface and Coatings Technology*, 275 (2015) pp.75-83.

[33] Moser, S., Dean Edwards, K., Schoeffler T., Filipi, Z., "CFD/FEA Co-Simulation Framework for Analysis of the Thermal Barrier Coating Design and Its Impact on the HD Diesel Engine Performance", *Energies*, vol. 14, no. 8, 2021. https://doi.org/10.3390/en14082044

[34] Motwani, R., Gandolfo, J., Gainey, B., Levi, A., Moser, S., Filipi, Z., Lawler, B., Assessing the Impact of a Novel TBC Material on Heat Transfer in a Spark Igntiion Engine through 3D CFD-FEA Co-simulation Routine," *SAE Technical Paper,* 2022. https://doi.org/10.4271/2022-01-0402

[35] Richards, K.K. Senecal, P.K. and Pomraning, E., *CONVERGE 3.0 Manual* (Madison, WI: Convergent Science, 2019)

[36] Liu, A. B., Mather, D., & Reitz, R. D. (1993). Modeling the effects of drop drag and breakup on fuel sprays. *SAE Transactions*, 83-95.

[37] Schmidt, D. P., & Rutland, C. J. (2000). A new droplet collision algorithm. *Journal of Computational Physics*, 164(1), 62-80

[38] Amsden, A.A., O'Rourke, P.J., and Butler, T.D., "KIVA-II: A Computer Program for Chemically Reactive Flows with Sprays," *Los Alamos National Laboratory Technical Report* LA-11560-MS, 1989.

[39] Reitz, R.D. and Bracco, F.V., "Mechanisms of Breakup of Round Liquid Jets," Encyclopedia

[40] Reitz, R.D., "Modeling Atomization Processes in High-Pressure Vaporizing Sprays," *Atomization and Spray Technology,* vol. 3, no. 4, 1987, p. 309-337.

[41] Reitz, R.D. and Diwakar, R., "Structure of High-Pressure Fuel Sprays," *SAE Paper* 870598, 1987. DOI: 10.4271/87059

[42] Turns, S.R., An Introduction to Combustion, McGraw-Hill, Inc., 1996

[43] Nagle, J., and Strickland-Constable, R.F., "Oxidation of Carbon Between 1000-2000 C," *Proceedings of the Fifth Carbon Conference*, Volume 1, Pergammon Press, 1962.184

[44] Hiroyasu, H. and Kadota, T., "Models for Combustion and Formation of Nitric Oxide and Soot in DI Diesel Engines," *SAE Paper* 760129, 1976. DOI: 10.4271/760129

[45] Smith, M., ABAQUS/CAE User's Manual, Version 6.14 (Dassault Systems Simulia Corp)

[46] ABAQUS documentation, https://ABAQUSdocs.mit.edu/2017/English/SIMACAEEXCRefMap/simaexc-c-docproc.htm

[47] Esfahanian, V., Javaheri, A., and Ghaffarpour, M., "Thermal Analysis of an SI Engine Piston Using Different Combustion Boundary Condition Treatments," *Applied Thermal Engineering* 26, no. 2-3 (2006): 277-287.

[48] Dahham, R., Wei, H., Pan, J., "Improving Thermal Efficiency of Internal Combustion Engines: Recent Progress and Remaining Challenges", *Energies* 2022, 15, 6222. https://doi.org/10.3390/en15176222

[49] Leach, F., Kalghatgi, G., Stone, R., Miles, P., "The scope for improving the efficiency and environmental impact of internal combustion engines", *Transportation Engineering*, vol. 1, 2020. https://doi.org/10.1016/j.treng.2020.100005

[50] Kumar, M., "A Finite Element Thermo-Mechanical Stress Analysis of IC Engine Piston," *International Research Journal of Engineering Technology* 4, no. 6 (2017): 1976-1981

[51] Gainey, B., Gandolfo, J., Yan, Z., Vedpathak, K., Kumar, R., H. Jordan, E., Sellnau, M., Filipi, Z., Lawler, B., "A two-material thermal barrier coating spatially tailored for high-efficiency GCI combustion", *International Journal of Engine Research*, 2023. https://doi.org/10.1177/14680874231194386

[52] Woschni, G., Spindler, W., Kolesa, K., “Heat Insulation of Combustion Chamber Walls — A Measure to Decrease the Fuel Consumption of I.C. Engines?”, *SAE Technical Paper*, vol. 96, no. 4, pp. 269-279, 1987. https://doi.org/10.4271/870339

[53] Andruskiewicz, P., Najt, P., Durrett, R., Biesboer, S., Schaedler T., Payri, R., “Analysis of the effects of wall temperature swing on reciprocating internal combustion engine processes”, International Journal of Engine Research, vol. 19, no. 4, 2017. https://doi.org/10.1177/1468087417717903